




Citicoline Modulates Glaucomatous Neurodegeneration Through Intraocular Pressure-Independent Control

Yolandi van der Merwe^{1,2} · Matthew C. Murphy^{1,3} · Jeffrey R. Sims⁴ · Muneeb A. Faiq⁴ · Xiao-Ling Yang¹ · Leon C. Ho¹ · Ian P. Conner^{1,2} · Yu Yu⁵ · Christopher K. Leung^{6,7} · Gadi Wollstein^{4,8} · Joel S. Schuman^{4,8,10} · Kevin C. Chan^{1,2,4,8,9,10} 

Accepted: 24 February 2021 / Published online: 13 April 2021
© The American Society for Experimental NeuroTherapeutics, Inc. 2021

Abstract

Glaucoma is a neurodegenerative disease that causes progressive, irreversible vision loss. Currently, intraocular pressure (IOP) is the only modifiable risk factor for glaucoma. However, glaucomatous degeneration may continue despite adequate IOP control. Therefore, there exists a need for treatment that protects the visual system, independent of IOP. This study sought, first, to longitudinally examine the neurobehavioral effects of different magnitudes and durations of IOP elevation using multi-parametric magnetic resonance imaging (MRI), optokinetics and histology; and, second, to evaluate the effects of oral citicoline treatment as a neurotherapeutic in experimental glaucoma. Eighty-two adult Long Evans rats were divided into six groups: acute (mild or severe) IOP elevation, chronic (citicoline-treated or untreated) IOP elevation, and sham (acute or chronic) controls. We found that increasing magnitudes and durations of IOP elevation differentially altered structural and functional brain connectivity and visuomotor behavior, as indicated by decreases in fractional anisotropy in diffusion tensor MRI, magnetization transfer ratios in magnetization transfer MRI, T1-weighted MRI enhancement of anterograde manganese transport, resting-state functional connectivity, visual acuity, and neurofilament and myelin staining along the visual pathway. Furthermore, 3 weeks of oral citicoline treatment in the setting of chronic IOP elevation significantly reduced visual brain integrity loss and visual acuity decline without altering IOP. Such effects sustained after treatment was discontinued for another 3 weeks. These results not only illuminate the close interplay between eye, brain, and behavior in glaucomatous neurodegeneration, but also support a role for citicoline in protecting neural tissues and visual function in glaucoma beyond IOP control.

Key Words Glaucoma · Citicoline · Intraocular pressure · Optokinetics · Magnetic resonance imaging · Visual system

✉ Kevin C. Chan
chuenwing.chan@fulbrightmail.org

¹ UPMC Eye Center, Eye and Ear Institute, Ophthalmology and Visual Science Research Center, Department of Ophthalmology, University of Pittsburgh, Pittsburgh, PA, USA

² Department of Bioengineering, Swanson School of Engineering, University of Pittsburgh, Pittsburgh, PA, USA

³ Department of Radiology, Mayo Clinic, Rochester, MN, USA

⁴ Department of Ophthalmology, NYU Grossman School of Medicine, NYU Langone Health, New York University, New York, NY, USA

⁵ Pleryon Therapeutics Limited, Shenzhen, China

⁶ University Eye Center, Hong Kong Eye Hospital, Hong Kong, China

⁷ Department of Ophthalmology and Visual Sciences, The Chinese University of Hong Kong, Hong Kong, China

⁸ Center for Neural Science, College of Arts and Science, New York University, New York, NY, USA

⁹ Department of Radiology, NYU Grossman School of Medicine, NYU Langone Health, New York University, New York, NY, USA

¹⁰ Neuroscience Institute, NYU Grossman School of Medicine, NYU Langone Health, New York University, New York, NY, USA

Introduction

Glaucoma is a neurodegenerative disease of the visual system that involves progressive retinal ganglion cell (RGC) death, optic nerve damage, and irreversible vision loss [1]. It is the second leading cause of blindness worldwide, with 60 million people suffering from glaucomatous optic neuropathy, of whom 8.4 million are blind [2]. One major risk factor for glaucoma is an increase in intraocular pressure (IOP). However, the direct causes of glaucoma are unknown, and it remains unclear how different degrees of IOP change affect glaucoma pathogenesis. Currently, the only effective way to slow down glaucoma progression is by decreasing IOP, despite the fact that degeneration of the visual system may still occur after lowering IOP to population-derived normal levels [3, 4]. Therefore, there exists a need for a better understanding of the disease mechanisms resulting from IOP elevation, as well as a treatment mechanism beyond lowering IOP in order to further decrease the severity of glaucoma and preserve or restore visual function.

To determine the mechanisms of disease progression in glaucoma, several animal models have been developed targeting different aspects of IOP-induced pathogenesis [5, 6]. However, many of these studies were performed *ex vivo* without visual outcome assessments, and the longitudinal effects of different degrees of IOP elevation on the visual system remain unclear. Recent studies also suggest that glaucoma may not only involve the eye, but also the brain in a trans-synaptic manner [7–12]. However, results remain controversial, partly due to small samples and limited methods available to probe properties of the eye, brain, and visual behavior *in vivo* and simultaneously [13]. There also remain barriers to determining if the brain can be the target for glaucoma therapeutics in addition to the eye. Development of a well-controlled, *in vivo* model system for longitudinal neurobehavioral analyses can help clarify mechanisms affecting vision loss in glaucoma patients and can provide a platform to evaluate the efficacy of novel glaucoma therapeutics. Therefore, in this study, we combined the use of experimental rat models of glaucoma, optokinetics, and advanced structural and functional magnetic resonance imaging (MRI) techniques to analyze the effects of acute and chronic IOP elevation on the visuomotor behavior response, white matter integrity, axonal transport, and functional connectivity between visual brain nuclei over time.

To explore treatment mechanisms that can reduce glaucomatous damage independent of IOP reduction, one may postulate strategies that can act to preserve neural tissues, promote neurorepair, improve vascular tone, and reduce functional loss across neurodegenerative diseases

and injuries. Among these candidates, citicoline (cytidine 5'-diphosphocholine) has been suggested to slow down the detrimental effects of Alzheimer's disease [14], traumatic brain injury [15], multiple sclerosis [16], cerebrovascular conditions, and cerebral ischemia [17] when administered exogenously. Citicoline is a non-toxic compound [18] that plays important roles in inhibiting phospholipid degradation and in synthesizing or repairing cell membrane [19]. It increases certain neurotransmitters such as dopamine, noradrenaline, and serotonin and serves as a choline donor in the biosynthesis of acetylcholine [20, 21]. Studies have also shown that citicoline may be neuroprotective in hyperglycemic conditions [22, 23], which is of further importance given research suggesting an association between insulin resistance and IOP elevation [24–26]. To date, the effects of citicoline on glaucomatous neurodegeneration remain unclear [27]. The effects of citicoline on the visual system have been explored initially through case control, prospective, and retrospective cohort studies [28–39]. Through activation of the dopaminergic system in the visual pathways, citicoline improves visual acuity, contrast sensitivity, and visually evoked potentials in patients with ischemic optic neuropathies [32, 40]. Studies involving cell culture and animal model systems have shown that citicoline plays vital role in improving neurite growth [41], imparting resistance to glutamate excitotoxicity [23], and preventing RGC death in optic nerve crush models [42] without significant alteration in IOP thereby making a case for its neuroprotective effects [38]. Several studies reported improvements in electrophysiology following intramuscular or oral citicoline administration [31, 32] with no significant difference in efficacy between the two routes. However, the effects generally returned to baseline after washout. These trials did not report visual field changes either. A related study observed ameliorating effects of oral citicoline on the progression of visual field damage compared with historical controls [29] but was limited to a relatively small sample size and lacked the follow-up data.

After oral ingestion, citicoline is hydrolyzed in the intestinal wall and liver to choline and cytidine, both of which are then rapidly absorbed, enter systemic circulation, cross the blood-brain barrier, enter the central nervous system, and reform as citicoline with over 90% bioavailability [20, 43]. In this study, we propose that oral citicoline treatment can ameliorate the effects of IOP elevation on glaucomatous damage and functional deterioration of the visual system. By using non-invasive, multi-parametric MRI and behavioral studies, it is possible to associate the degree of IOP elevation to longitudinal structural and functional changes in the visual system after experimental glaucoma induction and oral citicoline treatment. In this study, we used diffusion

tensor imaging (DTI) to characterize the microstructural fiber organization along the visual pathway by measuring water diffusion patterns in white matter compartments [44]. We also utilized magnetization transfer imaging (MTI) to examine changes in macromolecular structures, including myelin, by measuring the magnetization transfer ratio between water bound to macromolecules and the surrounding free water in the optic nerve [45]. Mn-enhanced MRI (MEMRI) was used to provide information regarding anterograde transport and the integrity of the axonal pathway after IOP elevation and oral citicoline treatment. Finally, resting-state functional connectivity MRI (RSfMRI) was used to explore the functional connectivity changes between brain regions throughout the visual system [46], whereas a subset of animals also underwent proton magnetic resonance spectroscopy ($^1\text{H-MRS}$) to examine choline metabolism in the visual cortex [47]. These multi-parametric brain MRI findings were examined alongside optokinetic and histological assessments using myelin basic protein (MBP) for myelination and phosphorylated neurofilament (pNF) for axonal integrity in order to determine how different magnitudes and durations of IOP elevation affect neurobehavioral outcomes with and without oral citicoline treatment.

The goals of this study were to examine neurobehavioral effects of different magnitudes and durations of IOP elevation via multi-parametric MRI, optokinetics, and histology and to evaluate neurotherapeutic effects of citicoline on experimental glaucoma. We hypothesized that differences in IOP elevation would induce different degrees of behavioral, structural, and functional brain changes, with more severe pathology in the setting of greater magnitudes and durations of IOP elevation and that citicoline may reduce or delay such effects in our chronic IOP elevation model without significantly altering IOP.

Methods

Study Design

All experiments were approved by the University of Pittsburgh Institutional Animal Care and Use Committee, and investigators followed guidelines from the Association for Research in Vision and Ophthalmology's statement for Use of Animals in Ophthalmic and Vision Research. A schematic of the experimental plan is provided in Fig. 1. In brief, eighty-two adult female Long Evans rats (Charles River Laboratories, Wilmington, MA) at about 8 weeks old were housed in a 12-h light/dark cycle with standard chow and water available *ad libitum* and were randomly assigned to six groups. All animals from each of the acute (mild or severe) IOP elevation, chronic (citicoline-treated or untreated) IOP elevation, and sham (acute or chronic) control groups

received neurobehavioral assessments using optokinetics (days 0, 7, 14, and 35), DTI (days 3, 7, 14, and 35), MTI (days 3, 7, 14, and 35), and RSfMRI (day 35). A subset of animals from the chronic IOP elevation and chronic sham groups also underwent $^1\text{H-MRS}$ (day 35). After RSfMRI and $^1\text{H-MRS}$, animals were randomly assigned for MEMRI (day 35) or histology (day 35) (Fig. 1a). The treated chronic IOP elevation animals received oral doses of citicoline daily for 7 days prior to IOP elevation induction and every 48 h for 14 days after IOP elevation induction. The acute groups had their IOP measured during experimental induction, whereas the chronic groups had their IOP measured at days 3, 7, 14, and 35 to verify that the IOP remained elevated for the duration of the experimental period.

Anesthesia

For all chronic IOP elevation induction, MR imaging procedures, and Mn contrast agent injection, animals were anesthetized via isoflurane inhalation (3% induction, 1.5% maintenance). To study acute IOP elevation induction, rats were anesthetized with an intraperitoneal injection of a 75:10 mg/kg ketamine/xylazine cocktail (Henry Schein, NY). All procedures were performed under sterile conditions, and rat body temperature was maintained and monitored using a circulating water blanket and a rectal thermometer. After experiments, animals were placed on a heating pad for recovery and monitored until fully conscious and ambulating.

Acute IOP Elevation Induction

Twenty-five animals received mild ($n=13$) or severe ($n=12$) acute IOP elevation in the right eye via physiological saline anterior chamber perfusion. The left eye remained untreated and served as an internal control. Proparacaine hydrochloride ophthalmic solution (Bausch & Lomb, Inc., Rochester, NY, USA) and tropicamide ophthalmic solution (Akorn, Lake Forest, IL) were topically applied to the right eye to induce analgesia and pupil dilation, respectively. A 30-gauge needle was connected to a sterile saline reservoir (0.9% sodium chloride; Baxter International Inc., Deerfield, IL, USA) via sterile tubing. The needle tip was inserted into the right eye's anterior chamber under a surgical microscope, parallel to the iris, taking care not to touch the iris or lens. Once inserted, the needle was secured in place to avoid movement during the experiment. IOP was elevated to 40 mmHg and 130 mmHg for mild and severe acute IOP elevation, respectively, by elevating the saline reservoir to the appropriate height. The reservoir was secured in place for 60 min and IOP was measured with both a handheld rebound tonometer (Icare TonoLab, Finland) and a pressure transducer (BIOPAC Systems, Goleta, CA, USA) connected

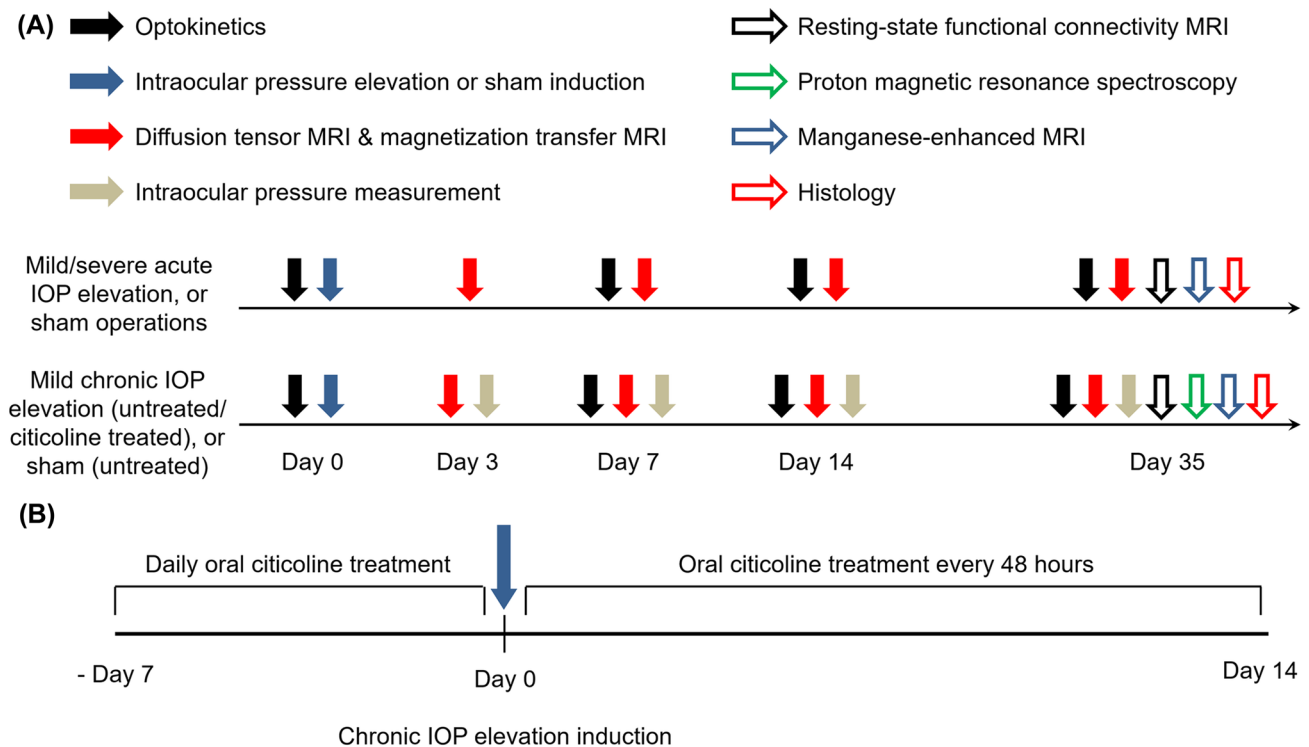


Fig. 1 Experimental paradigm. **(a)** Experimental timeline for measuring eye, brain, and behavioral changes following acute (top) and chronic (bottom) intraocular pressure (IOP) elevation or sham operations across 5 weeks. Vertical arrows represent visuomotor behavior measurements through optokinetics (solid black), intraocular pressure elevation or sham induction (solid blue), diffusion tensor imaging (DTI), and magnetization transfer imaging (MTI) using 9.4 T MRI (solid red), IOP measurements through tonometry (solid gray), resting-state functional connectivity MRI (RSfcMRI) (black outline),

metabolic proton magnetic resonance spectroscopy (green outline), anterograde transport through manganese-enhanced MRI (MEMRI) (blue outline), and histology (red outline). **(b)** Treatment paradigm for oral citicoline administration. A subgroup of animals in the chronic IOP elevation group received oral citicoline treatment at a dose of 500 mg/kg body weight. Animals received daily citicoline administration for 7 days prior to IOP elevation induction, and every 48 h for 14 days following chronic IOP elevation induction.

in line with sterile tubing. Afterwards, the reservoir was lowered, and the needle was removed from the anterior chamber. Antibiotic ointment (Gentamicin, Akorn, Lake Forest, IL) was applied topically immediately after removal of the needle. Sham procedures ($n=9$) to mild and severe acute IOP elevation were performed by cannulating the right eye as described and keeping the saline reservoir at eye level for 60 min.

Chronic IOP Elevation Induction

Thirty-eight animals received an intracameral injection of an optically clear cross-linking hydrogel into the anterior chamber of the right eye to induce chronic IOP elevation [48]. The left eye remained uninjected and untreated, serving as an internal control. Proparacaine and tropicamide were first topically applied to the right eye to induce analgesia and pupil dilation. The right eye was injected intracamerally with 15 μ L of a 1:1 mixture of 4% vinyl sulfonated hyaluronic acid and 4% thiolated hyaluronic acid [48–50]. The injections were performed under a surgical

microscope with a microinjection system through a glass micropipette (World Precision Instruments, Sarasota, FL, USA). The solidified hydrogel obstructed aqueous outflow, thereby causing a sustained increase in IOP. Antibiotic ointment was applied topically immediately after injection. Sham procedures to the hydrogel-induced glaucoma model were performed on 10 animals by injecting only phosphate-buffered saline (PBS) solution into the right anterior chamber. IOP was measured with the handheld TonoLab tonometer at days 3, 7, 14, and 35 after intracameral injection to verify if the IOP elevation was sustained.

Citicoline Administration

Among the 38 animals that received chronic IOP elevation induction, 19 of them also received daily citicoline treatment (500 mg/kg [16]; Jarrow Formulas, Los Angeles, CA) via oral gavage for 7 days prior to chronic IOP elevation induction, and every 48 h for 14 days after chronic IOP elevation induction. Citicoline was freshly diluted in saline before each treatment.

Optokinetics

The OptoMotry virtual-reality optokinetic system (Cerebral-Mechanics Inc., Lethbridge, Alberta, Canada) [51] was used to assess visuomotor behavior by quantifying the visual acuity of each eye. Animals were acclimated to the system once per day for 3 days prior to data collection. Acclimation sessions lasted 20 min, during which the animals were exposed to stimuli similar to those presented during data collection. During data collection, spatial frequency ranged from 0.042 to 0.750 cycles/degree using a simple staircase method while rotation speed (0.12°/s) and 100% contrast were maintained throughout the experiment.

MRI Protocols

All MR imaging was performed using a 9.4-T/31-cm Varian/Agilent horizontal MRI scanner (Santa Clara, CA, USA) with a 38-mm diameter transmit-receive volume coil and a receive surface coil.

DTI was acquired for all animals using a fast spin-echo sequence with 12 diffusion gradient directions at $b = 1.0 \text{ ms}/\mu\text{m}^2$ and 2 non-diffusion-weighted images at $b = 0 \text{ ms}/\mu\text{m}^2$ (b_0). Other imaging parameters included repetition time/echo time (TR/TE) = 2300/27.8 ms, echo train length = 8, diffusion gradient duration time (δ)/diffusion gradient separation time (Δ) = 5/17 ms, field of view = $2.6 \times 2.6 \text{ cm}^2$, acquisition matrix = 192×192 (zero-filled to 256×256), 20 1-mm thick slices, and 4 repetitions. Slices were oriented orthogonal to the prechiasmatic optic nerves.

MTI was acquired for all animals at the level of the prechiasmatic optic nerves at the same orientation and time points as DTI with 9.5- μT saturation pulses at 4000 Hz off-resonance. Other parameters included TR/TE = 1500/8.43 ms, echo train length = 8, field of view = $2.6 \times 2.6 \text{ cm}^2$, acquisition matrix = 192×192 (zero-filled to 256×256), one 1-mm thick slice, and 2 repetitions.

Manganese (Mn) ions are paramagnetic and can act as a calcium analog that enters voltage-gated calcium channels followed by active anterograde transport along axonal pathways via microtubules [52]. In this study, MEMRI was performed on a randomly selected subset of the mild acute IOP elevation ($n = 9$), severe acute IOP elevation ($n = 9$), acute sham control ($n = 6$), untreated chronic IOP elevation ($n = 12$), citicoline-treated chronic IOP elevation ($n = 13$), and chronic sham control ($n = 6$) groups. Each animal received binocular intravitreal injections of 1.5 μL of 100 mM manganese chloride (MnCl_2) after all other imaging and behavioral studies were completed. T1-weighted images were acquired before and at 8 h after MnCl_2 injections with a fast spin-echo sequence. The same geometric parameters were used as for DTI, with TR/TE = 600/8 ms, echo train length = 8, and 8 1-mm thick slices. A saline

syringe phantom was placed next to the animal head for signal normalization to account for potential system instability between imaging sessions.

For RSfMRI, T2-weighted images were first acquired to serve as an anatomical reference. A single-shot gradient-echo echo-planar imaging sequence was then used for each session, with TR/TE = 2000/18 ms, field of view = $32 \times 32 \text{ mm}^2$, acquisition matrix = 64×64 , six 1-mm thick slices, and 420 repetitions. Each session lasted about 14 min, and 4 sessions were acquired per animal, resulting in approximately 1 h of total scan time per animal.

^1H -MRS was acquired in a subset of animals in the untreated chronic IOP elevation ($n = 6$), citicoline-treated chronic IOP elevation ($n = 7$), and chronic sham control ($n = 7$) groups. A $4 \times 4 \times 1 \text{ mm}^3$ voxel was placed over the left and right visual cortices (VC) [53] each, centering on gray matter while avoiding underlying white matter structures and the skull. The water signal was suppressed with variable power radiofrequency pulses with optimized relaxation delays (VAPOR), and the spin echo full-intensity acquired localized (SPECIAL) spectroscopy sequence [54] was used for signal acquisition. Other parameters included TR/TE = 4000/4.04 ms, averages = 512, data points = 4096, and spectral bandwidth = 8013 Hz.

Histology

Animals not receiving Mn injections were sacrificed at the terminal point for histology. They were euthanized with an intraperitoneal injection of 50 mg/kg pentobarbital and whole-body perfusion was used to fix the tissue for histology. When the animals no longer responded to a toe pinch, they were perfused with PBS at pH 7.4, followed by 4% paraformaldehyde in PBS. Optic nerves were harvested and fixed for an additional 48 h in 4% paraformaldehyde in PBS at 4 °C. Samples were placed in 30% sucrose for cryoprotection, and then embedded in optical cutting temperature medium. The optic nerves were sectioned into 10- μm thick sections, placed on histology slides, and kept at $-20 \text{ }^\circ\text{C}$ until use.

Sections were stained for phosphorylated neurofilament (pNF) (1:1000, Covance, NJ, USA) and myelin basic protein (MBP) (1:50, Santa Cruz Biotechnology, TX, USA). The sections were washed three times with PBS and were blocked and permeabilized overnight with 0.2% Triton X-100, 1% bovine serum albumin (BSA), and 5% donkey serum in PBS. pNF and MBP primary antibodies were diluted to working concentrations in 1% BSA and 5% donkey serum in PBS and incubated for 3 days at 4 °C. The sections were washed three times in PBS and incubated with secondary antibodies (1:500 donkey anti-goat Alexa488 for MBP, 1:500 donkey anti-mouse Alexa546 for pNF) in 1% BSA in PBS for 2 h at room temperature. Sections were

rinsed in PBS, stained with 4',6-diamidino-2-phenylindole (DAPI), and imaged with a confocal microscope (Olympus Fluoview1000, Tokyo, Japan) at 60× magnification with the same exposure times used across sections for each antibody.

Data Analysis

All data analysis was completed with blinding with respect to the experimental group. For DTI, SPM8 (Wellcome Department of Imaging Neuroscience, University College, London, UK) was used for co-registration between diffusion-weighted and non-diffusion-weighted images. A total of 3×3 diffusion tensors were placed on non-diffusion-weighted and diffusion-weighted images on a pixel-by-pixel basis using DTIStudio v3.02 (Johns Hopkins University, Baltimore, MD). Maps of DTI-derived parameters including fractional anisotropy (sensitive to overall microstructural integrity), axial diffusivity (sensitive to axonal integrity), and radial diffusivity (sensitive to myelin integrity) were computed using eigenvectors and eigenvalues in DTIStudio to assess the resultant structural integrity of the visual pathway after IOP elevation and oral citicoline treatment. Regions of interest were drawn manually using ImageJ v1.47 (Wayne Rasband, NIH, USA) at the prechiasmatic optic nerves at Bregma + 1.5 mm, and the optic tracts at Bregma – 3.5 mm based on the fractional anisotropy directionality map, fractional anisotropy value map, axial and radial diffusivity maps, and the rat brain atlas [55]. The corresponding DTI parametric values were then extracted. As more than 90% of the optic nerve fibers in adult rodents decussate at the optic chiasm to the contralateral optic tract [52], the visual pathway projecting from the injured right eye (right optic nerve and left optic tract) was assessed relative to that projecting from the uninjured left eye (left optic nerve and right optic tract), followed by between-group comparisons over time.

For MTI, the magnetization transfer ratio for the prechiasmatic optic nerve was calculated as $(M_0 - M_{\text{sat}})/M_0$, where M_{sat} represents the magnetization signal with saturation pulse, and M_0 represents the magnetization signal without saturation pulse. Regions of interest were manually drawn on the prechiasmatic optic nerve and quantified using ImageJ.

For MEMRI, T1-weighted signal intensities in the left and right optic nerves, lateral geniculate nuclei (LGN), and superior colliculi (SC) were measured using manual regions of interest drawing in ImageJ. Signal intensities were normalized to the nearby saline phantom to counter for system instability between imaging sessions. Differences in Mn enhancement between injured and uninjured visual pathways were quantified by calculating the percentage difference in normalized T1-weighted signal intensities in the right optic nerve, left LGN, and left SC relative to the left optic nerve, right LGN, and right SC, respectively.

For ^1H -MRS, MR spectra were analyzed using jMRUI v5.2 (MRUI Consortium, <http://www.jmrui.eu/>)%20 (56, 57). Residual water signal was filtered out using the Hackel-Lanczos singular value decomposition (HLSVD) algorithm. Metabolite areas were calculated using quantitation-based quantum estimation (QUEST) with subtraction modeling to remove background signal, and the choline levels were normalized to creatine (Cr) to account for systematic fluctuations between experimental sessions. The reliability of values obtained was verified with Cramer-Rao lower bounds (CRLB) below 25% [58].

For IOP, optokinetics, and MRI assessments other than RSfMRI, results are presented as mean \pm standard error of mean (SEM). Analysis of variance was used in conjunction with a Tukey's post hoc test to determine significance between groups using GraphPad Prism v5.00 (GraphPad Software Inc., La Jolla, CA, USA). Results were considered significant when $p < 0.05$.

For RSfMRI, images were realigned to the first volume to account for small head motions using a 3 degree-of-freedom rigid body transformation (translations in the imaging plane and rotations about the slice direction). The images were then smoothed with a 2D Gaussian function with a standard deviation of 2 voxels, followed by a temporal ideal bandpass filter with cutoff frequencies of 0.01 and 0.1 Hz. Finally, the effects of motion were regressed out of the signal using the motion parameters estimated during realignment, as well as the first- and second-order temporal derivatives of the motion parameters. Before this regression step, the motion parameters were also temporally filtered as above to avoid the reintroduction of high-frequency noise into the preprocessed data. Regions of interest were drawn manually on the LGN, SC, and VC in each hemisphere, beginning with the first run of data for each animal and then propagated to all remaining runs by performing a 3-degree-of-freedom transformation between the first images of each pair of runs, thereafter applying this transformation to the drawn regions of interest. Functional connectivity in each run was then summarized by computing the mean time course in each region, computing the Pearson correlation between each pair of time courses, and converting these correlation coefficients to z-score using the Fisher r-to-z transformation. In this way, each run of data was summarized by a graph where the regions of interest define the nodes and the strength of the correlation between a given pair of regions of interest defines the edges. For each edge in the graph, effects for group-wise differences were investigated using a linear mixed-effects model with random slopes and intercepts included for each animal. We then performed an *F*-test on each group, with a false discovery rate corrected $Q < 0.05$ considered significant. Where the *F*-tests were significant, post hoc testing was performed with analogous mixed-effects models but with data restricted to the two groups being compared.

Results

IOP Elevation Was Induced at Different Magnitudes and Durations with No Effects from Citicoline

For the acute IOP elevation groups, the target IOP level was confirmed with both a handheld rebound tonometer (Icare Tonolab, Finland) and a pressure transducer (BIOPAC Systems, Goleta, CA, USA) that was connected in line with sterile tubing during anterior chamber perfusion (Fig. 2a). The same handheld tonometer was used to

confirm successful induction of chronic IOP elevation. As shown in Fig. 2b, intracameral hydrogel injection into the right eye significantly elevated IOP throughout the experimental period. In both citicoline-treated and untreated groups, the IOP of the right eye steadily increased from day 3 to day 14 and remained unchanged from day 14 to day 35. No significant IOP difference was observed between citicoline-treated and untreated animals. IOP remained unchanged over the experimental period in the left uninjured eye of the experimental groups, as well as both eyes of the sham groups.

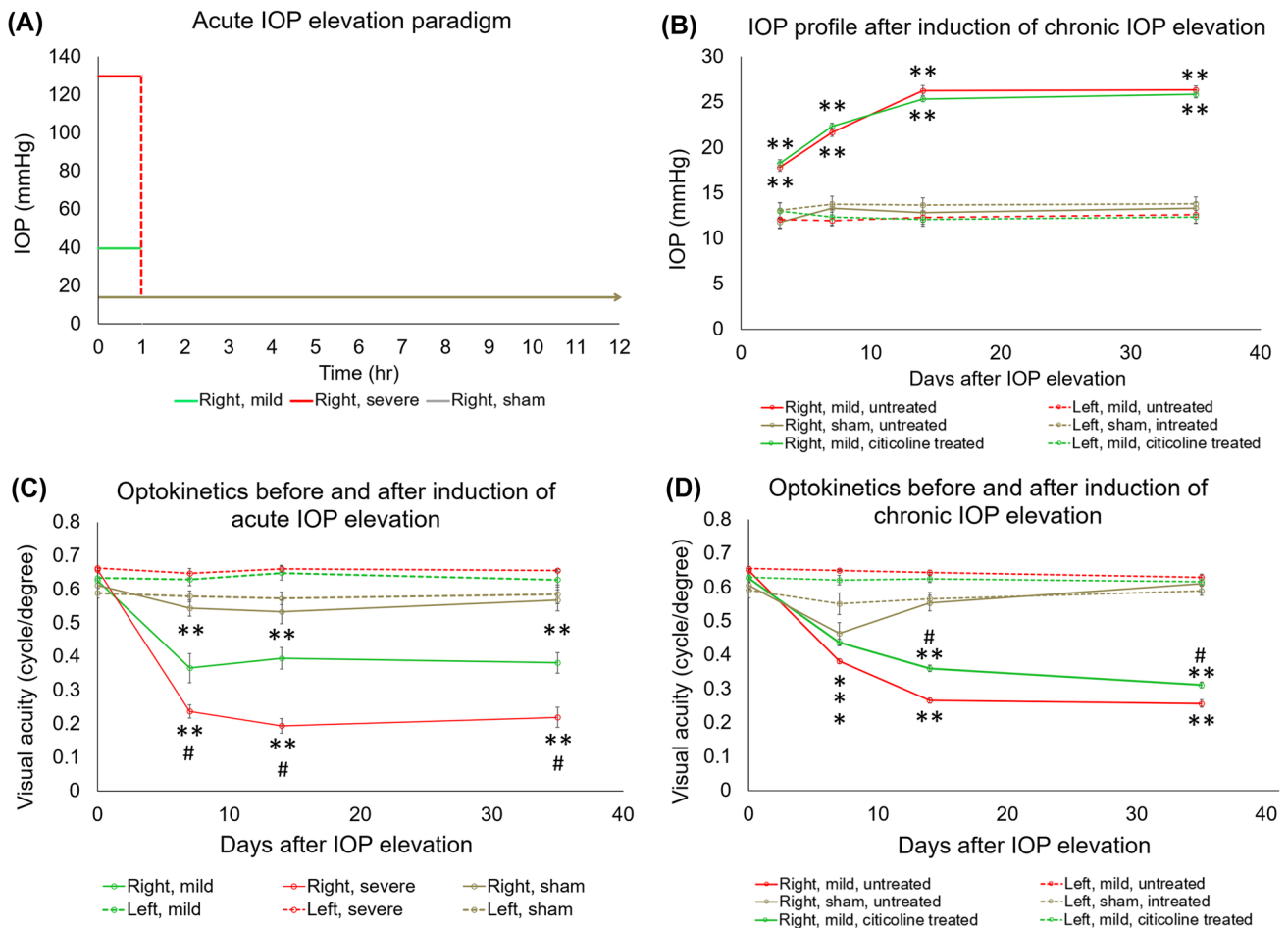


Fig. 2 Intraocular pressure (IOP) profiles (**a**, **b**) and visual acuity (VA) (**c**, **d**) in acute (**a**, **c**) and chronic (**b**, **d**) groups. (**a**) Anterior chamber perfusion to the right eye elevated IOP for 1 h, after which IOP returned to baseline physiological level. (**b**) Hydrogel injection to the right eye elevated IOP for the duration of the experimental period, with no significant IOP difference between citicoline-treated and untreated animals. (**c**, **d**) VA of the left eyes remained unchanged and was comparable with the right eyes before IOP elevation. (**d**) The VA of the right eyes of both acute IOP elevation groups was

decreased compared with the left eyes at days 7, 14, and 35, and VA of the severe group was decreased compared with the mild group at days 7, 14, and 35. (**d**) The worsening in VA of the right eyes of citicoline-treated and untreated animals started at day 7 and was slower for the citicoline-treated group compared with the untreated group. Post hoc Tukey's tests between left and right eyes, $*p < 0.05$, $**p < 0.01$; in right eyes between mild and severe groups ($\#p < 0.05$); and in right eyes between treated and untreated groups ($\#p < 0.05$). Data are represented as mean \pm SEM.

Acute and Chronic IOP Elevation Decrease Visual Acuity, While Citicoline Slows Down This Progression

Using optokinetic behavioral assessments, the visual acuity of the left uninjured eye in all groups remained unchanged over time and was comparable with the right experimental eye before IOP elevation (Fig. 2c, d). The visual acuity of the right experimental eye significantly decreased from pre-injury (day 0) to day 7 after both mild and severe acute IOP elevation and continued to be significantly lower than the visual acuity of the left eye at days 14 and 35 (Fig. 2c). At days 7, 14, and 35, the right experimental eye under severe acute IOP elevation had a significantly lower visual acuity than that under mild acute IOP elevation (Fig. 2c).

The right eye in all chronic groups showed a significant visual acuity decrease of varying extents from day 0 to day 7 (Fig. 2d). By day 14, the right eye of the sham group had apparently recovered, with no visual acuity difference between left and right eyes at days 14 and 35. In contrast, the right eye of both the citicoline-treated and untreated groups showed a progressive decrease in visual acuity at days 14 and 35. However, despite similar levels of IOP elevation, right eye visual acuity was significantly higher in the citicoline-treated group, compared with the untreated group, at both of these time points (Fig. 2d).

Diffusion Tensor MRI of White Matter Integrity After IOP Elevation and Oral Citicoline Treatment

When examining the microstructural integrity of the visual pathways projecting from the right experimental eye and the left uninjured eye using longitudinal DTI (Figs. 3 and 4), among the acute groups (Fig. 3), severe acute IOP elevation resulted in a significantly larger fractional anisotropy decrease in the optic nerve at day 35 compared with sham procedures (Fig. 3b). The optic nerve also showed a significantly larger radial diffusivity increase at day 35 after severe acute IOP elevation compared with the sham control (Fig. 3d). Over the time course, significant progression in fractional anisotropy decrease and radial diffusivity increase was observed in the optic nerve after severe acute IOP elevation when comparing days 3 and 7 with day 35. Statistically significant trends were not observed in the optic tract (Fig. 3e–g).

Following untreated chronic IOP elevation (Fig. 4), the optic nerve showed significantly larger fractional anisotropy and axial diffusivity decreases at days 7 and 35 when compared with the sham control (Fig. 4b, c). Furthermore, the untreated optic nerve showed a significantly larger radial diffusivity increase at days 7, 14, and 35 when compared with the sham group (Fig. 4d). The optic tract in the untreated chronic IOP elevation group had a significantly greater radial diffusivity increase at days 14 and 35 when compared with

the sham group (Fig. 4g). When treated with citicoline, the optic tract showed a significantly smaller fractional anisotropy decrease at days 14 and 35 compared with the untreated chronic IOP elevation group (Fig. 4e). No significant difference in DTI parametric values was observed between citicoline-treated chronic IOP elevation and sham control groups along the visual pathway (Fig. 4b–g).

Magnetization Transfer MRI of White Matter Integrity After IOP Elevation and Oral Citicoline Treatment

When examining the macromolecular contents of the optic nerves using longitudinal MTI (Fig. 5), among the acute groups (Fig. 5a and c), the optic nerve showed an early decline in magnetization transfer ratio at day 3 after severe acute IOP elevation. The decline was significantly larger than that in the mild acute IOP elevation group and was significantly larger than the sham control group until the end experimental time point. Among the chronic groups (Fig. 5b and d), chronic IOP elevation without citicoline treatment resulted in a significantly larger decrease in magnetization transfer ratio in the optic nerve when compared with that with citicoline treatment at both days 14 and 35, whereas the magnetization transfer ratio was significantly different between untreated chronic IOP elevation and sham control groups at day 35. No significant magnetization transfer ratio difference in the optic nerve was observed between citicoline-treated chronic IOP elevation and sham control groups throughout the experimental period.

Manganese-Enhanced MRI of Axonal Transport After IOP Elevation and Oral Citicoline Treatment

In order to quantify the anterograde Mn transport along the visual pathways projecting from the right experimental eye [i.e., right optic nerve, left lateral geniculate nucleus (LGN), and left superior colliculus (SC)] and from the left uninjured eye (i.e., left optic nerve, right LGN, and right SC), T1-weighted signal intensities of these brain regions were measured before and at 8 h following intravitreal injection of MnCl₂ into both eyes at the end experimental time point on day 35 (Fig. 6). Before intravitreal Mn injection, no significant difference in T1-weighted signals was observed along the visual pathways between hemispheres in either acute or chronic groups.

When assessing the percent intensity difference between injured and uninjured visual pathways after bilateral intravitreal Mn injection, among the acute groups (Fig. 6b–d), the left LGN showed a significantly larger reduction in Mn enhancement after severe acute IOP elevation compared with mild acute IOP elevation and sham control (Fig. 6c). The left SC also showed a significantly larger reduction in

Diffusion tensor MRI following acute IOP elevation

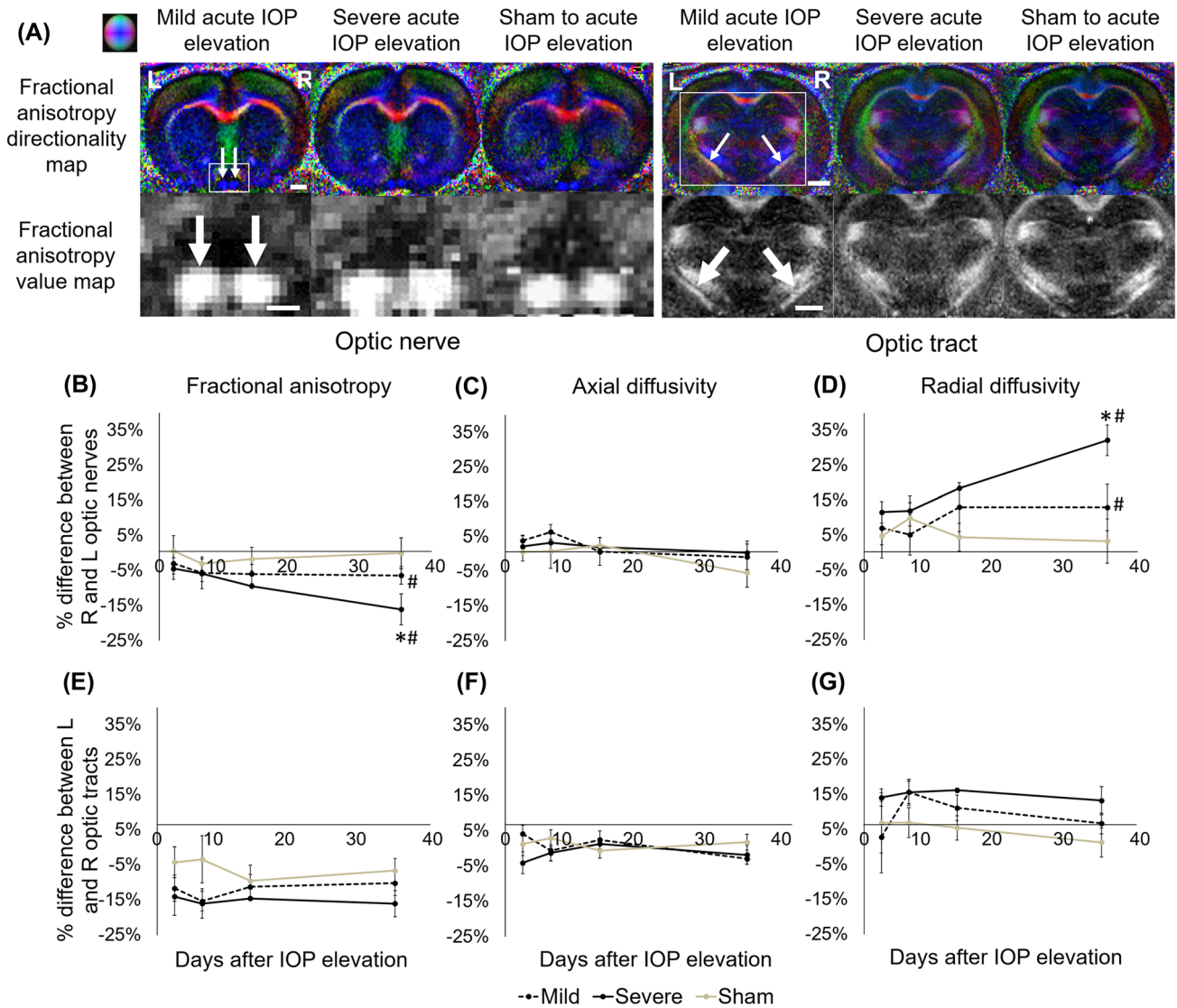


Fig. 3 Diffusion tensor imaging (DTI) of the optic nerve and optic tract following acute IOP elevation or sham operations over time. **(a)** Representative fractional anisotropy directionality (color) and value (grayscale) maps in the optic nerve and optic tract in mild acute IOP elevation, severe acute IOP elevation, and sham injury animals at day 35. White arrows indicate optic nerves and the optic tracts, and white boxes indicate the area magnified in the second row. Color representations for the principal diffusion directions: blue, caudal-rostral; red, left-right; green, dorsal-ventral. **(b–g)** Results are quantified and

shown as percentage difference in fractional anisotropy (FA), axial diffusivity (AD), or radial diffusivity (RD) between injured and uninjured optic nerves and tracts, and the percentage differences are compared between groups. Comparing severe and sham injury groups at day 35, there were significant differences in **(b)** FA and **(d)** RD in the optic nerves (post hoc Tukey's tests, $*p < 0.05$). FA and RD in the optic nerves in the mild and severe groups were also significantly different between day 35 and days 3 and 7 (post hoc Tukey's tests, $\#p < 0.05$). Data are represented as mean \pm SEM. Scale bar = 2 mm.

Mn enhancement after severe acute IOP elevation compared with sham control (Fig. 6d).

Among the chronic groups (Fig. 6e–g), the right optic nerve, left LGN, and left SC showed a significantly larger reduction in Mn enhancement after untreated chronic IOP elevation compared with sham control (Fig. 6e–g), whereas

the left LGN showed a significantly smaller reduction in Mn enhancement after citicoline-treated chronic IOP elevation compared with untreated chronic IOP elevation (Fig. 6f). No significant difference in Mn enhancement was observed between citicoline-treated chronic IOP elevation and sham control groups in the optic nerve or the LGN (Fig. 6e–g).

Diffusion tensor MRI following chronic IOP elevation

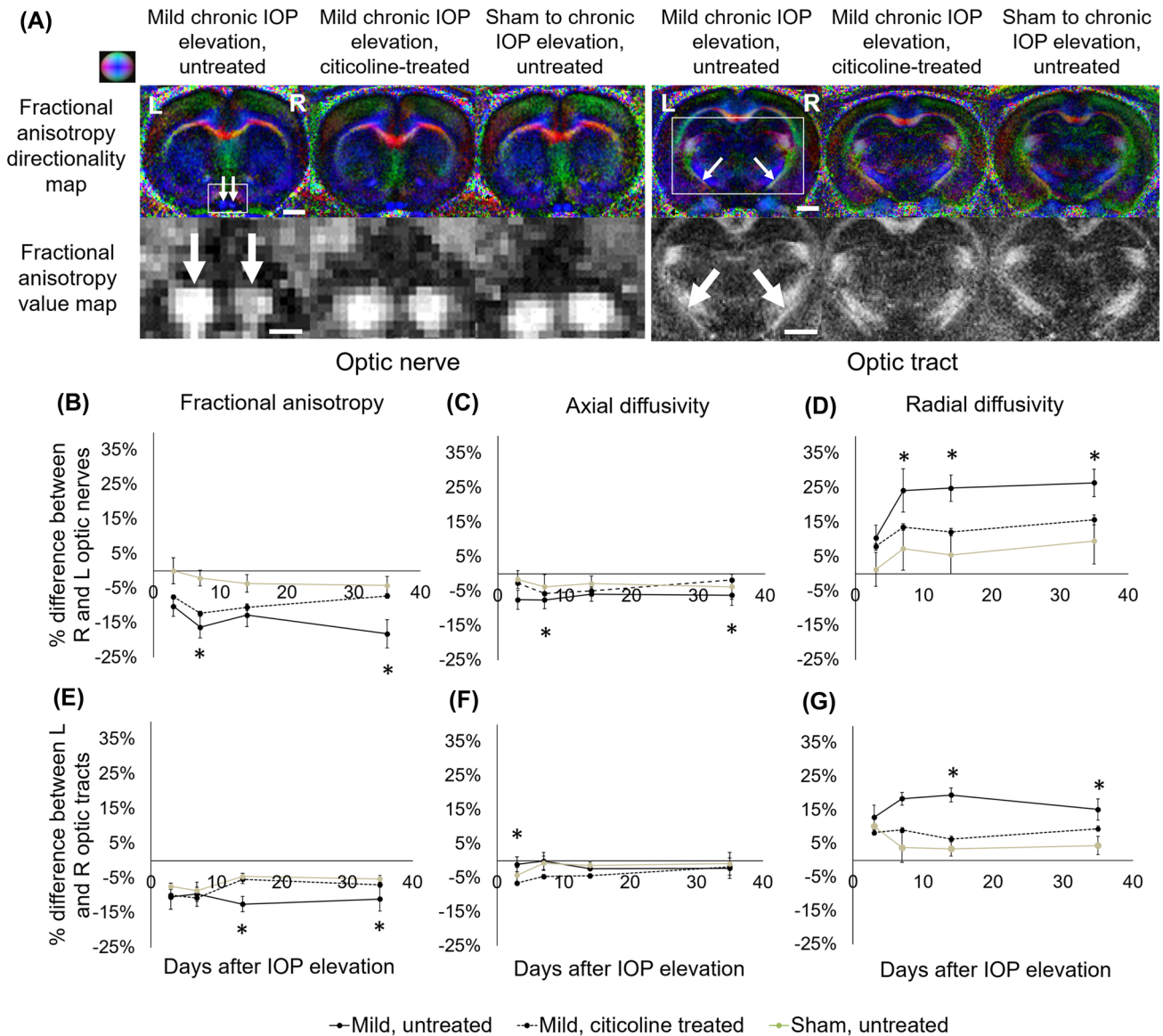


Fig. 4 Diffusion tensor imaging (DTI) of the optic nerve and optic tract following chronic IOP elevation or sham operations over time. **(a)** Representative fractional anisotropy directionality (color) and value (grayscale) maps in the optic nerve and optic tract in untreated chronic IOP elevation, citicoline-treated chronic IOP elevation, and untreated sham injury groups at day 35. Color representations for the principal diffusion directions: blue, caudal-rostral; red, left-right; green, dorsal-ventral. **(b–g)** Results are quantified and shown

as percentage difference in fractional anisotropy (FA), axial diffusivity (AD), or radial diffusivity (RD) between injured and uninjured optic nerves and tracts, and the percentage differences are compared between groups. **(b–g)** At various time points, there were significant differences in FA, AD, and RD between the untreated and sham injury groups, which were seen in both the optic nerves and optic tracts. Post hoc Tukey’s tests, $*p < 0.05$. Data are represented as mean \pm SEM. Scale bar = 2 mm.

Functional Connectivity MRI of the Visual System After IOP Elevation and Oral Citicoline Treatment

When comparing the resting-state functional connectivity between the LGN, SC, and visual cortex [53] of each hemisphere, significant functional connectivity differences were observed in the subcortical visual nuclei between all

three acute groups, with greater differences across increasing magnitudes of IOP elevation (Fig. 7a). Among the chronic groups, animals with untreated chronic IOP elevation showed significantly decreased cortico-collicular, cortico-geniculate, and subcortical functional connectivity compared with the sham control both intra- and inter-hemispherically (Fig. 7b). In contrast, animals that received chronic IOP elevation

Magnetization transfer MRI following acute and chronic IOP elevation

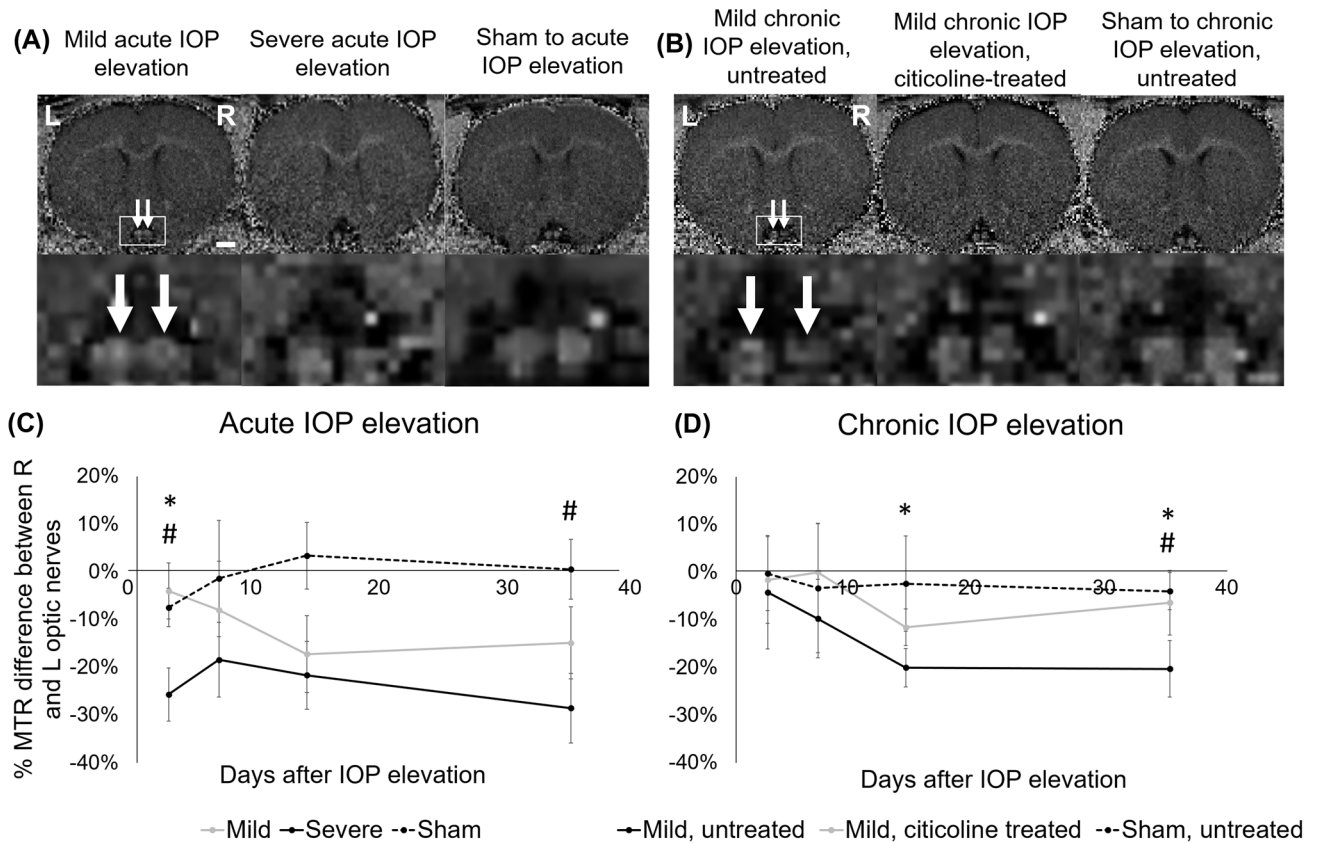


Fig. 5 Magnetization transfer imaging (MTI) of the optic nerve (white arrows) following acute (a, c) and chronic (b, d) IOP elevation or sham operations. (a, b) Representative magnetization transfer ratio (MTR) maps of the optic nerve at day 35. (c, d) Results are quantified and shown as percentage MTR difference between injured and uninjured optic nerves, and the percentage differences are compared between groups. (c) There were significant differences between mild and severe groups at 3 days after acute IOP elevation (post hoc

Tukey's tests, $*p < 0.05$), and between severe and sham groups at 3 and 35 days after acute IOP elevation ($\#p < 0.05$). (d) There were also significant differences between untreated and citicoline-treated groups at 14 and 35 days after chronic IOP elevation. Post hoc Tukey's tests, $*p < 0.05$, and between untreated and sham groups at 35 days after chronic IOP elevation, $\#p < 0.05$. Data are represented as mean \pm SEM. Scale bar = 2 mm.

and oral citicoline treatment appeared to have preserved or increased functional connectivity. Compared with untreated chronic IOP elevation, the citicoline-treated group also had increased functional connectivity between the left VC and left SC.

¹H-MRS of Visual Cortex Metabolism Following Chronic IOP Elevation and Oral Citicoline Treatment

Five weeks after hydrogel or sham buffer injection into the right eye, ¹H-MRS of the untreated chronic IOP elevation group demonstrated significantly lower choline levels in the left VC corresponding to the right injected eye than in the right VC corresponding to the left uninjured eye (Fig. 8). In the citicoline-treated chronic IOP elevation group, choline levels were not significantly different between the left

and right VC. However, the left VC in the citicoline-treated group had significantly higher choline levels than that in the untreated chronic IOP elevation and sham injected groups. No significant difference in choline levels was found in the right VC among the three chronic groups.

Histological Assessment Following IOP Elevation and Oral Citicoline Treatment

Immunohistochemical staining for phosphorylated neurofilament (pNF) and myelin basic protein (MBP) showed comparable expression in the left uninjured optic nerve across all groups (Fig. 9a, b). The pNF staining was decreased by $43.6 \pm 3.6\%$ and $65.7 \pm 0.7\%$ in the right optic nerve of the mild and severe acute IOP elevation groups, respectively, compared with the left optic nerve (Fig. 9c). In the chronic

Manganese-enhanced MRI following acute and chronic IOP elevation

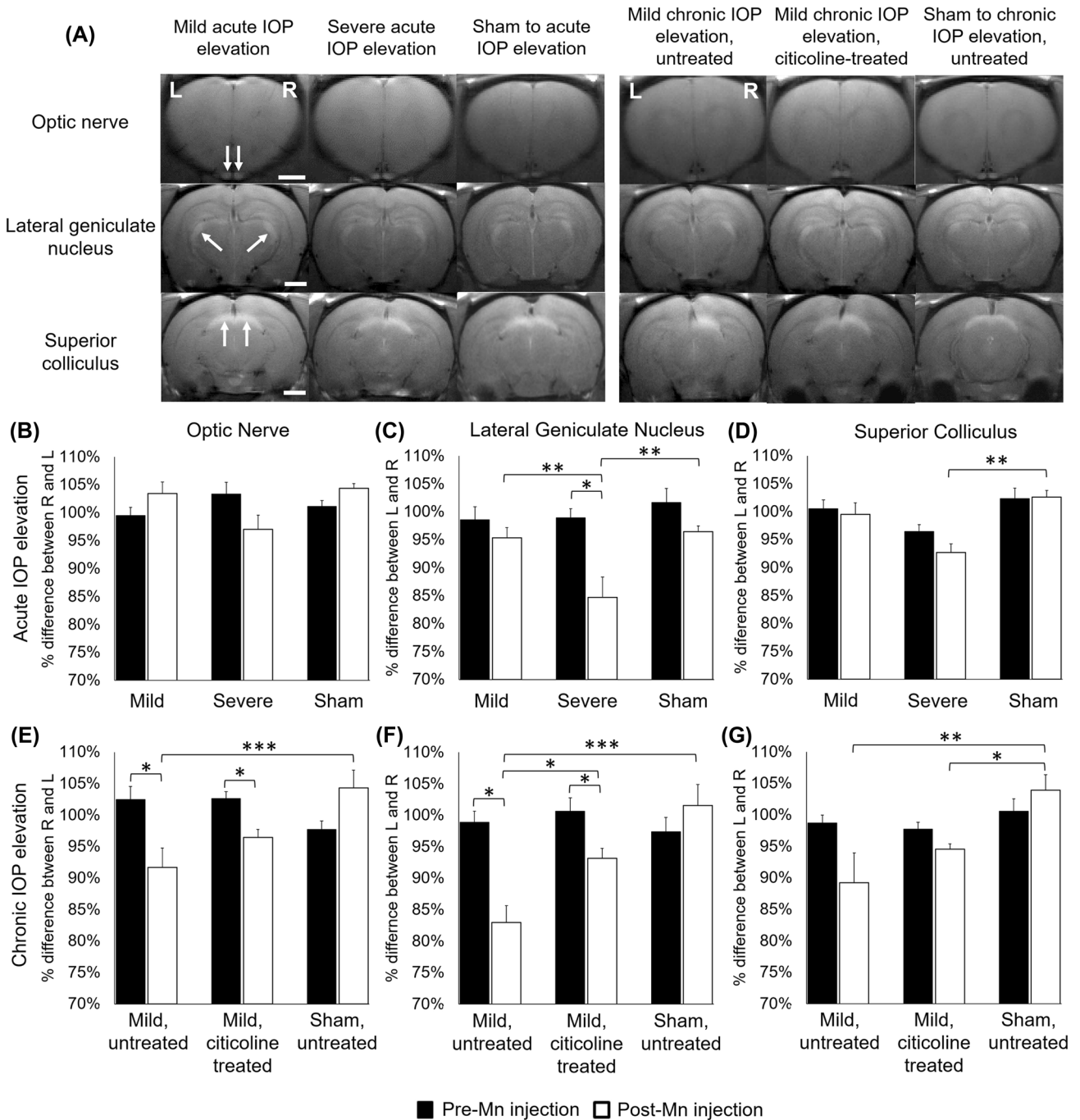


Fig. 6 Manganese-enhanced MRI (MEMRI) of anterograde manganese transport at 35 days after acute and chronic IOP elevation or sham operations. **(a)** Representative post-Mn injection images in the optic nerve (top row), lateral geniculate nucleus (LGN) (middle row), and superior colliculus (SC) (bottom row) at 8 h after intravitreal MnCl₂ injection into both eyes. White arrows indicate manganese

enhancement. **(b)** Percent difference in T1-weighted signal intensities was calculated between injured and uninjured optic nerves, LGN, and SC and was compared between groups and between pre- and post-Mn injection. Post hoc Tukey's tests, **p* < 0.05, ***p* < 0.01, ****p* < 0.001. Data are represented as mean ± SEM. Scale bar = 2 mm.

IOP elevation groups, the pNF staining in the right optic nerve was decreased by $64.4 \pm 1.4\%$ in the untreated group and by $43.6 \pm 3.5\%$ in the citicoline-treated group (Fig. 9d). The MBP staining was decreased in the right optic nerve of the mild and severe acute IOP elevation groups by $24.6 \pm 4.2\%$ and $65.1 \pm 1.0\%$, respectively, compared with the left optic nerve (Fig. 9e). In the chronic IOP elevation groups, the MBP staining in the right optic nerve was decreased by $59.4 \pm 2.9\%$ and $38.3 \pm 4.2\%$ in the untreated and citicoline-treated groups, respectively, compared with the left optic nerve (Fig. 9f).

Discussion

Our current understanding of how to treat glaucoma and prevent further permanent damage to the visual system is almost exclusively directed at reducing IOP. For example, IOP-lowering procedures like trabeculectomies and laser trabeculoplasties have the potential to preserve visual function in some glaucoma patients [59, 60]. However, IOP reduction has variable short-term and long-term efficacy in patients with glaucoma, which may decrease quality of life. Given our growing knowledge of the ways glaucomatous degeneration affects different areas of the visual system, there is a strong desire to monitor such changes and to find agents with neurotherapeutic roles to alleviate and prevent such damage.

The present study demonstrates that different levels of acute and chronic IOP elevation cause varying degrees of structural, functional, and behavioral changes in the visual system. Furthermore, such neurobehavioral effects can be modulated via oral citicoline treatment without significantly affecting the magnitude of IOP elevation. These experiments have important implications for both our understanding of glaucomatous degeneration and the ways in which we may be able to prevent such neurodegenerative processes. Given the variety of experimental techniques used in this study, it is possible to elucidate the effects of increased IOP and citicoline treatment on different aspects of neurologic health, including axon integrity and visual system functionality.

By comparing results across DTI, MTI, and histological studies, we gain a better understanding of consequences of glaucomatous change relevant to the brain's visual system. In DTI, increased radial diffusivity is sensitive to demyelination, while decreased axial diffusivity may reflect axonal degeneration [61]. In the acute IOP elevation groups, which experienced IOP elevation for only one hour, progressive changes were observed in optic nerve fractional anisotropy and radial diffusivity for up to 5 weeks after injury. The increase in radial diffusivity and decrease in MBP morphology staining were more pronounced in severe than mild acute IOP elevation, suggesting that higher IOP elevation causes a larger disruption in myelin density. In the chronic

groups, a gradual increase in radial diffusivity and late changes in fractional anisotropy and axial diffusivity were also found in the visual pathway after unilateral anterior chamber hydrogel injection, indicating that neurodegeneration occurs progressively over the course of chronic IOP elevation. These changes did not occur when animals received citicoline treatment. Interestingly, while oligodendrocyte loss and demyelination have been thought to occur late in the progression of glaucomatous degeneration, recent studies in glaucoma patients and animal models demonstrated early glial involvements relative to axonal degeneration [62, 63], which supports the current findings. MTI allows for the detection of changes in macromolecular structures along the visual pathway [45] and complements the DTI findings. In particular, as greater myelin content often results in a higher magnetization transfer ratio, the smaller reduction in magnetization transfer ratio observed in the citicoline-treated group suggests that citicoline treatment after IOP elevation can inhibit changes in white matter myelination on a molecular level. Together with the histological findings of improved MBP density after oral citicoline treatment, these experiments support roles of both duration and magnitude of IOP elevation in visual pathway injury, the possibility that citicoline preserves vision by altering myelination amongst others, and the sensitivity of DTI and MTI in detecting such neurodegenerative and neuroprotective processes.

The effects of acute and chronic IOP elevation on axonal integrity were also examined via DTI, MEMRI, and histological studies. MEMRI can be used to examine physiological anterograde Mn transport in the retina and the brain's visual pathway [52, 64, 65] and has previously been shown to be capable of indicating injury severity in an optic nerve crush model [66]. In the acute groups, although decreased pNF-positive staining was observed in the right optic nerve at increasing levels of acute IOP elevation, there were no observable differences in axial diffusivity or Mn transport in the optic nerve. This supports the notion that axial diffusivity is related to Mn transport [67], and that axial diffusivity and MEMRI findings may reflect more than neurofilament integrity [52, 68, 69]. Following chronic IOP elevation alone, the optic nerve, LGN, and SC all showed significantly greater Mn transport deficits, as well as decreased axial diffusivity, when compared with the sham injury group. Conversely, the citicoline-treated group showed significantly smaller Mn transport deficits in the LGN compared with the untreated group, while the untreated group had significantly decreased pNF density compared with the sham and citicoline treated groups, suggesting that citicoline had protective effects on these axons. These results provide further evidence that chronic IOP elevation disrupts axon integrity, potentially causing decreased anterograde transport in the visual system. In congruence with the DTI, MTI, and histological findings, citicoline treatment appears to preserve

Resting-state functional connectivity MRI following acute and chronic IOP elevation

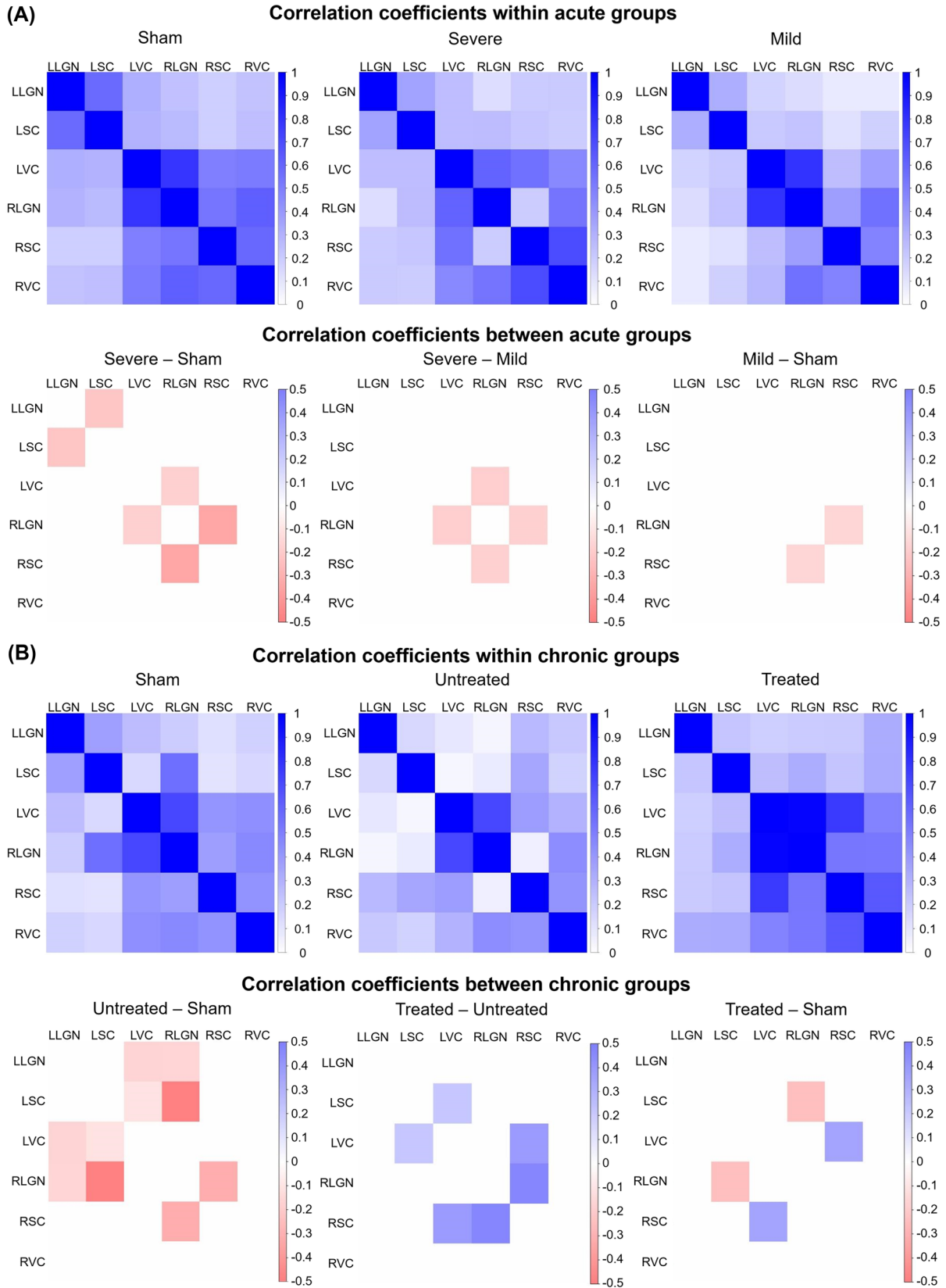


Fig. 7 Resting-state functional connectivity MRI (RSfMRI) at 35 days after acute (a) or chronic (b) IOP elevation or sham operations. (a) RSfMRI at 35 days after acute IOP elevation induction at physiological level (sham), 40 mmHg (mild), and 130 mmHg (severe). Top row indicates the visual brain functional connectivity (FC) as represented by the correlation strengths between lateral geniculate nucleus (LGN), superior colliculus (SC), and visual cortex [53] of the left (L) and right (R) hemispheres in each acute group. Bottom row represents the FC differences between acute groups. (b) RSfMRI at 35 days after chronic IOP elevation induction with (treated) or without (untreated) oral citicoline treatment, or sham operations (sham) without oral citicoline treatment. Top row represents the FC between LGN, SC, and VC of the L and R hemispheres in each chronic group. Bottom row represents the FC differences between chronic groups. For both (a) and (b), only statistically significant FC differences are colored in the bottom row.

anterograde Mn transport and protect white matter integrity in the setting of chronic IOP elevation.

Apart from the above structural interpretations of the MRI findings, it is important to note that the current MRI results could also be considered to be due, in part, to vascular status. One of the underlying components of normal-tension glaucoma pathophysiology is vascular endothelial dysfunction, particularly affecting the microvasculature [70] and blood flow in the retina and optic nerve, as well as the visual cortex. This vascular endothelial component may be explained by Flammer syndrome studies [71, 72] which demonstrated vascular autoregulation [73, 74] modulation by the cholinergic system [75, 76]. The retina is metabolically active and highly dependent on the precise regulation of blood supply for nutrients and oxygenation. Vascular deficits and consequent ischemia/hypoperfusion may thus be etiologically related to glaucoma [76, 77]. This notion has been confirmed by studies exploring vascular regulation in the retina and the optic nerve [73, 78, 79]. Furthermore, reduced vascular caliber in the retina [80] and atrophy of the peripapillary capillaries that supply the inner retina are associated with glaucoma [72]. This is interestingly related to Flammer syndrome, as a strong association between glaucoma and endothelin dysregulation has been reported in both normal-tension and open angle glaucoma [71, 81]. While it has been established that mental stress affects cholinergic neurotransmission in the brain [82], dysfunction of the acetylcholine system has been found to precipitate anxiety [27], with concomitant elevation in cortisol levels [83]. Cortisol upregulation has been shown to be associated with vascular dysregulation and endothelial dysfunction-mediated glaucoma [70, 84, 85]. Altogether, these findings suggest an interrelated network of processes including microvasculature regulation, the cholinergic system, and Flammer syndrome in the maintenance of the visual system. Studies focusing on this component of glaucoma have shown encouraging results [86, 87]. In order to understand

how the observed MRI changes in the optic nerve affected vision on functional and physiological levels, optokinetic behavioral performance, resting-state functional connectivity, and choline metabolism were examined. In contrast to the stable findings in the acute sham group and in the left uninjured eyes, animals in the acute IOP elevation groups had decreased visual acuity in the right experimental eyes that worsened with increasing IOP. In the chronic sham group involving intravitreal PBS injection, the initial decrease in visual acuity at day 7 recovered by day 14, while no prolonged effects on visual acuity or structural MRI were observed. This supports the notion that intraocular PBS injection is not toxic to the retina [88]. On the other hand, the citicoline-treated and untreated chronic IOP elevation groups had a progressive decline in visual acuity that persisted to days 14 and 35. Of note, visual acuity remained significantly higher in animals that received citicoline treatment compared with those with untreated chronic IOP elevation, even after ceasing citicoline treatment at day 14. This is consistent with the imaging and histological results that demonstrated long-lasting effects of citicoline on structural integrity of the visual pathways, and these findings suggest that citicoline has the potential to protect visual function sustainably without directly affecting IOP.

Studies have shown that glaucoma affects functional connectivity in the human brain [89]. Previous studies in mouse models have also shown that IOP elevation may permanently decrease synaptic connections and neural activity despite neurons appearing histologically healthy [11]. In the current RSfMRI experiments, it was found that oral citicoline preserved functional connectivity between the SC, LGN, and VC after chronic IOP elevation. Studies utilizing acetylcholinesterase inhibitors, which prevent acetylcholine hydrolysis and increase the concentration and duration of acetylcholine in the central nervous system, have demonstrated an increase in functional connectivity, visual perception, and processing in healthy subjects [90, 91], as well as enhanced brightness discrimination capacity after optic nerve crush [92]. Likewise, our ¹H-MRS findings show that chronic IOP elevation causes a significant decrease in choline metabolism in the visual cortex projecting from that eye. Furthermore, oral citicoline administration under chronic IOP elevation resulted in significantly higher visual cortex choline levels than untreated IOP elevation, suggesting that citicoline can replenish choline metabolism in the setting of glaucomatous damage and potentially treat such metabolic derangements. The higher choline levels in the left VC of the citicoline-treated group than the sham group may also suggest hyperactive physiologic changes in the brain tissue in response to injury and treatment, though the exact mechanisms driving this improvement above baseline level

Proton magnetic resonance spectroscopy following chronic IOP elevation

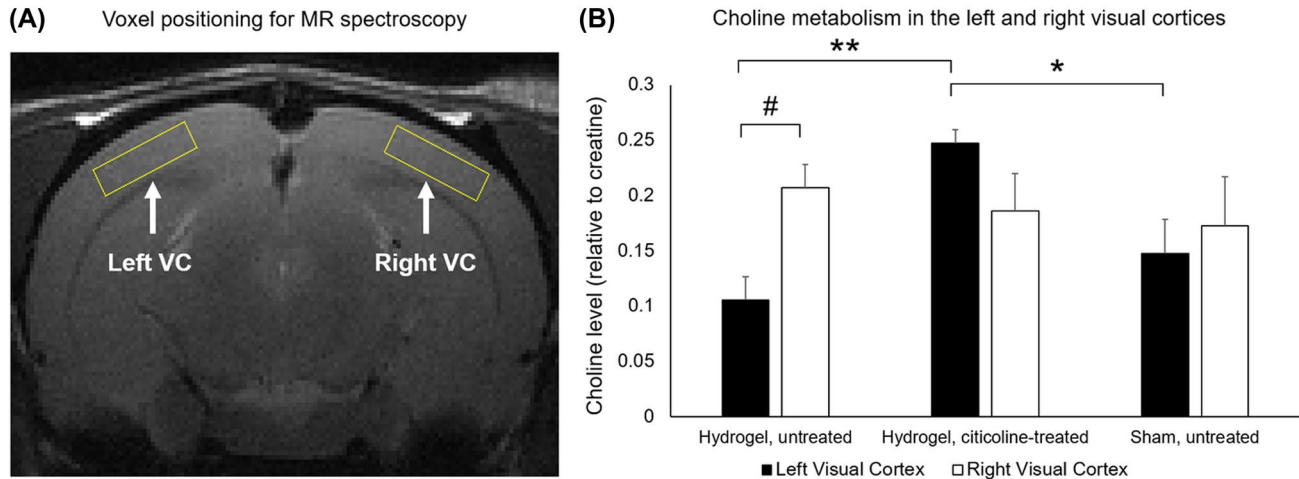


Fig. 8 Proton magnetic resonance spectroscopy (^1H -MRS) of choline levels in the visual cortex (VC) of the chronic groups 5 weeks after hydrogel or sham injection into the right eye. **(a)** Sample localization of $4 \times 4 \times 1 \text{ mm}^3$ MRS voxels over the left and right visual cortices [53] on T2-weighted MRI. **(b)** Quantification of choline-containing metabolites in the left and right VC for hydrogel-injected/untreated, hydrogel-injected/citicoline-treated, and sham-injected/untreated animals. Choline levels were normalized to creatine (Cr) to account for systematic fluctuations between experimental sessions. In the hydrogel-injected/untreated chronic IOP elevation group, the left

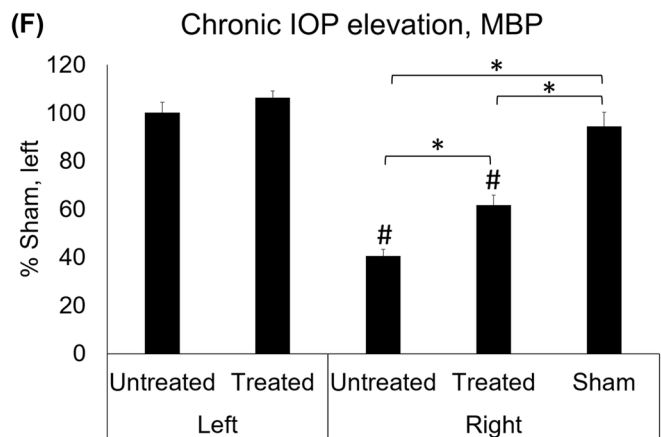
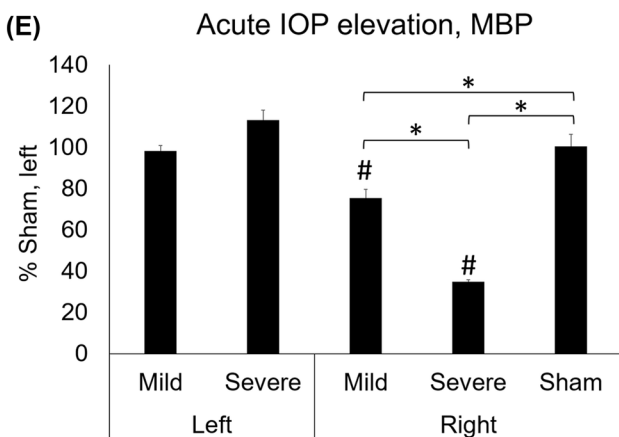
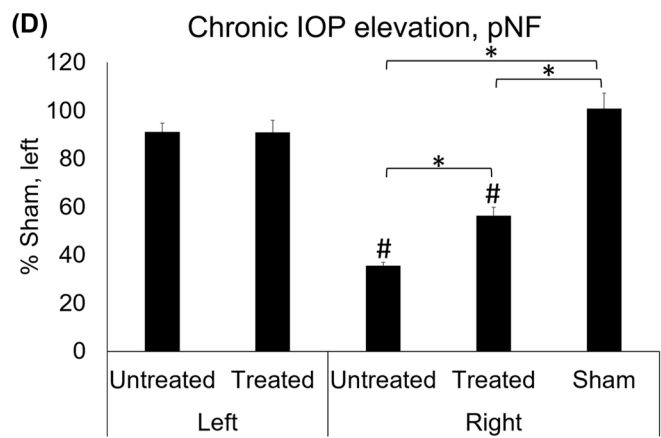
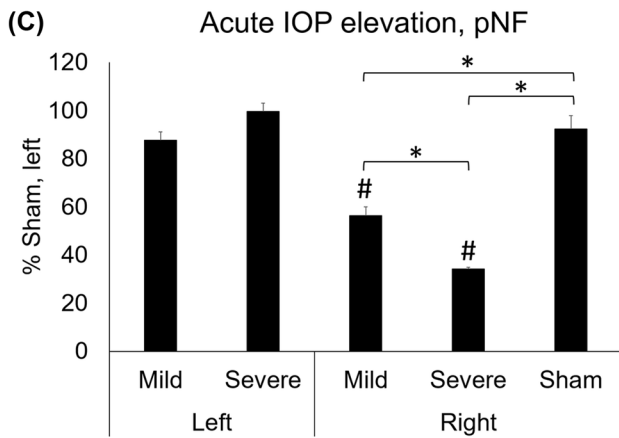
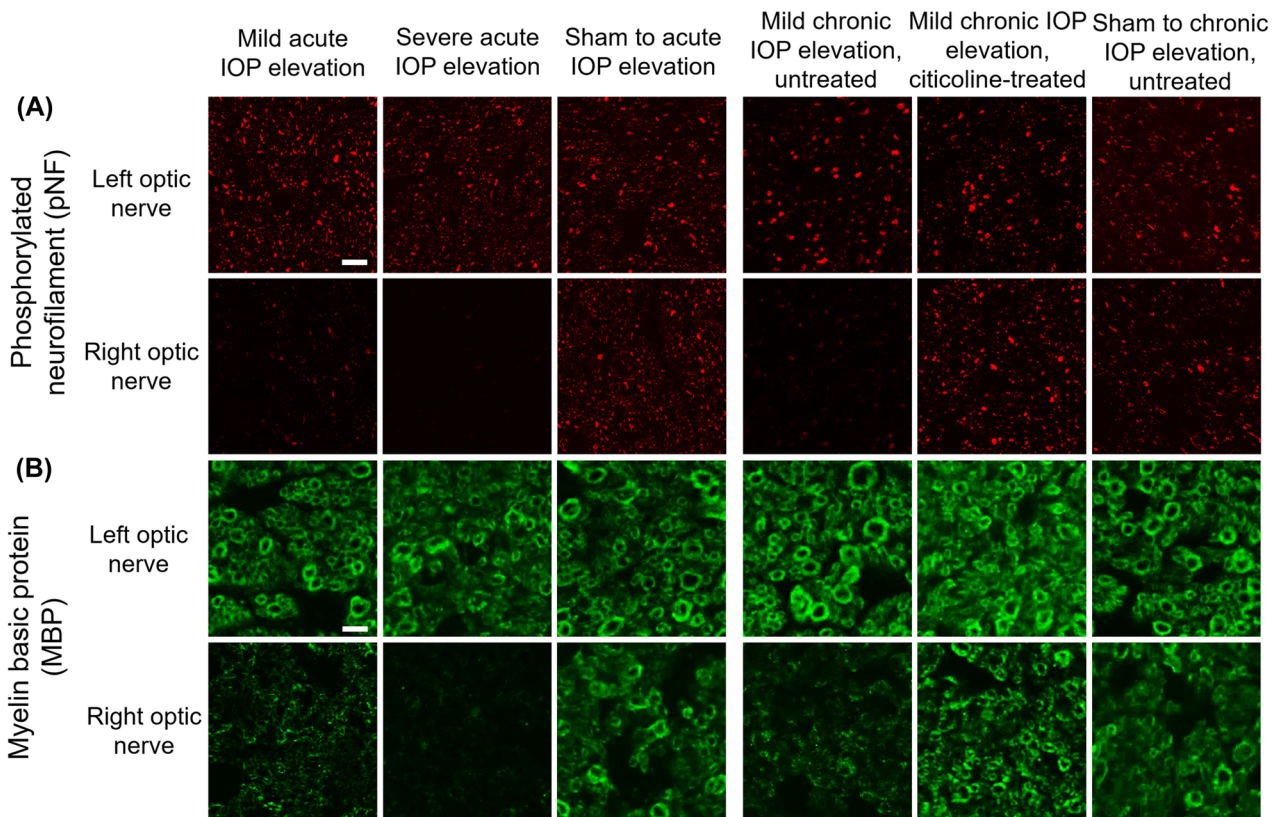
VC had significantly lower choline contents compared with the right VC. In contrast, the left VC projecting from the injected right eye of the citicoline-treated chronic IOP elevation group had significantly higher choline levels compared with the untreated chronic IOP elevation group and the sham group. There was no significant difference in choline contents between the 3 chronic groups in the right VC that corresponded to the left uninjured eye. Post hoc Tukey's tests between groups, $*p < 0.05$, $**p < 0.01$, and paired t tests between left and right VC, $\#p < 0.01$. Data are represented as mean \pm SEM.

require further testing in larger studies. Taken together, these results suggest that increased citicoline in the brain may improve functional connectivity and cortical physiology in the visual system in the setting of injury or disease.

It is important to note that choline metabolism involves a balance between binding to cytidine monophosphate and acetylation [53, 93]. Acetylation is the preferred metabolic pathway since it allows for functional utilization of the molecule [94]. In the event of restricted choline availability, either due to restricted supply or rapid depletion, phosphatidylcholine is hydrolyzed in response to the choline deficiency [95]. Citicoline, therefore, exerts effects by being a source of choline for synthesis of acetylcholine and rescue repertoire for phosphatidylcholine and other membrane component degradation [39]. This can help prevent neuronal membrane breakdown and apoptosis, thereby potentially providing neuroprotection. Taken in the context of glaucomatous and other optic neuropathies, citicoline can be thought to address three domains: protection of undamaged, rescue of partially damaged, and regeneration of substantially damaged RGCs and axons. While there is no distinct boundary between these processes, recent findings together with our current observations suggest that citicoline may act through a combination of these mechanisms [27].

Limitations and Future Directions

The current experiments were able to examine how citicoline can improve neuronal repair following the onset of IOP elevation, with measurable improvement in visual acuity, white matter integrity, anterograde Mn transport, functional brain connectivity, and visual cortical metabolism. To date, the efficacy of citicoline treatment in glaucoma patients remains variable across studies and the exact mechanisms of such findings remain unclear [27]. The experiments in this study can be used to help us better understand the therapeutic and prophylactic benefits of citicoline and other prospective therapeutics prior to administration in humans. There are, nevertheless, certain limitations for the experiments in the present study. Since the untreated chronic IOP elevation group did not receive the saline vehicle via oral gavage, there is no control for direct effects of gastric feeding in the citicoline-treated group, nor was there caloric measurement. In future experiments, we can include these additional controls to examine for any impact of the gastric feeding procedure or nutrition. The present study was performed exclusively in female rats. While some research has suggested that estrogen may have protective effects on RGCs, studies have largely shown insignificant effects of hormonal fluctuations during the menstrual cycle on IOP [96, 97]. All



◀ **Fig. 9** Phosphorylated neurofilament (pNF) and myelin basic protein (MBP) staining at 35 days after acute and chronic IOP elevation or sham operations. (a, b) Representative images of (a) pNF and (b) MBP staining in the optic nerve at 35 days after IOP elevation. (c–f) Quantitative comparisons relative to the left optic nerve in sham groups. Mild and severe acute IOP elevation decreased (c) pNF and (e) MBP positive staining compared with sham controls, with severe acute IOP elevation causing a significantly larger decrease in positive staining compared with mild acute IOP elevation. Under chronic IOP elevation, both citicoline-treated and untreated groups had significantly decreased (d) pNF and (f) MBP positive staining compared with the sham group, while citicoline-treated chronic IOP elevation had significantly smaller decrease in positive staining than untreated chronic IOP elevation. Post hoc Tukey's tests between groups, * $p < 0.05$, and compared with the left eye of sham control, # $p < 0.05$. Data are represented as mean \pm SEM. Scale bar = 20 μ m.

animals in this study were young adult age-matched female animals, making any impact of differences in cumulative estrogen exposure or timing in the estrous cycle during measurements unlikely. To determine the effects of sex on glaucoma neurotherapeutics, male animals will be included in future experiments.

There are important technical considerations for the experimental modalities used in this study. Previous research has shown that Mn may be toxic to neural pathways [52], meaning that histology should only be performed using samples from animals that were not used for MEMRI experiments. On the other hand, since retinal apoptosis and retinal ganglion cell death may affect Mn uptake in the retina, MEMRI findings may reflect not only changes in anterograde Mn transport but also damage to the retina. On a positive note, the improved Mn enhancement along the visual pathway after citicoline treatment suggested preserved connections not only in the brain but also the eye, including the retina. In future studies, longitudinal scans over hours can be taken after intravitreal Mn injection to determine the rate of Mn transport along the visual pathway and further elucidate the validity of these findings. Generally speaking, DTI is a sensitive imaging modality but has a relatively lower specificity under *in vivo* experimental conditions. The addition of MEMRI and MTI in this study improved the specificity of the DTI observations and provided complementary *in vivo* biomarkers to further explain the axonal and myelin integrity in our experimental models. Since pathology ranging from inflammation to gliosis can cause diffusion MRI changes apart from demyelination and axonal degeneration, higher-order diffusion imaging that can differentiate isotropic and anisotropic diffusion changes may allow for greater specificity in future experiments [68, 69]. The present study also does not rule out the possibility of changes in blood flow regulation, which can be affected by citicoline, driving some of the results observed on MRI. Future experiments may use additional imaging techniques to more directly examine the morphology of the optic nerve head, before and

after treatment, to control for any effects of morphometry and stereology.

In this study, the dosing and route of administration were chosen based on prior studies in other neurodegenerative diseases [16], while pre- and post-conditioning were used in an attempt to maximize pharmacologic effects prior to future refinement of the treatment schedule. Given the flexibility of the experimental paradigm in this study, parameters such as dosage, timing, and route of delivery could easily be modified and further optimized for more effective citicoline treatment. By expanding our experimental paradigm to be longer than 35 days, it would also be possible to study longer-term effects of citicoline treatment, as well as better evaluate our hydrogel model of chronic IOP elevation. Similarly, we plan on testing citicoline treatment in acute IOP elevation, as well. Whereas optic nerve histology was performed to validate the *in vivo* imaging findings in this study, further experiments with histological assessment of the entire visual pathway will provide a more comprehensive understanding of the consequences of elevated IOP. Histology was completed at the end experimental time point, largely as an initial proof of concept for the presence of optic nerve changes and confirmation of the sensitivity of the *in vivo* imaging findings. Future studies will include histology at each time point to more comprehensively understand the pathophysiological changes in these tissues. Future studies may also employ normal tension glaucoma animal models, such as transgenic optineurin E50K and TBK1 mice to examine how citicoline affects glaucoma pathogenesis and recovery fully independent of IOP [98]. Furthermore, it is possible that IOP-lowering strategies combined with neurotherapeutics can further protect visual neurons in the retina and brain, which may help to preserve vision in patients with glaucoma more effectively. Future experimentation utilizing both traditional IOP reduction and delivery of therapeutics like citicoline could lay the foundation for multifaceted treatment regimens for these patients.

Conclusions

In this study, a variety of experimental modalities were employed in order to better understand the pathophysiology of the visual system in the setting of glaucomatous degeneration, as well as to examine the possibility of intervention and neuroprotection independent of IOP alteration. Both magnitude and duration of IOP elevation were demonstrated to affect the structure and function of the visual system. Additionally, citicoline was shown to be capable of reducing these effects sustainably without altering IOP elevation. This study provides a framework and experimental

paradigm for longitudinal monitoring of the neurodegenerative events of the visual system in glaucoma and provides the groundwork for characterizing the restorative roles of neurotherapeutic treatment options in glaucoma.

Supplementary Information The online version contains supplementary material available at <https://doi.org/10.1007/s13311-021-01033-6>.

Required Author Forms [Disclosure forms](#) provided by the authors are available with the online version of this article.

Funding This work was supported in part by the National Institutes of Health R01-EY028125 (Bethesda, Maryland); BrightFocus Foundation G2019103 (Clarksburg, MD, USA); Liesegang Fellowship (New York, New York); Research to Prevent Blindness/Stavros Niarchos Foundation International Research Collaborators Award (New York, New York); and an Unrestricted Grant from Research to Prevent Blindness to NYU Langone Health Department of Ophthalmology. The funders above did not have any involvement in the study design, data collection, data analysis, interpretation, or manuscript writing.

References

- Danesh-Meyer HV, Levin LA. Glaucoma as a neurodegenerative disease. *J Neuroophthalmol*. 2015;35 Suppl 1:S22-S28.
- Tham YC, Li X, Wong TY, et al. Global prevalence of glaucoma and projections of glaucoma burden through 2040: a systematic review and meta-analysis. *Ophthalmology*. 2014;121(11):2081-2090.
- Susanna R, Jr., De Moraes CG, Cioffi GA, et al. Why Do People (Still) Go Blind from Glaucoma? *Transl Vis Sci Technol*. 2015;4(2):1.
- Cohen LP, Pasquale LR. Clinical characteristics and current treatment of glaucoma. *Cold Spring Harb Perspect Med*. 2014;4(6).
- Morrison JC, Johnson E, Cepurna WO et al. Rat models for glaucoma research. *Prog Brain Res*. 2008;173:285-301.
- Weinreb RN, Lindsey JD. The importance of models in glaucoma research. *J Glaucoma*. 2005;14(4):302-304.
- Yucel Y, Gupta N. Glaucoma of the brain: a disease model for the study of transsynaptic neural degeneration. *Prog Brain Res*. 2008;173:465-478.
- Sponsel WE, Groth SL, Satsangi N, et al. Refined Data Analysis Provides Clinical Evidence for Central Nervous System Control of Chronic Glaucomatous Neurodegeneration. *Transl Vis Sci Technol*. 2014;3(3):1.
- Crish SD, Sappington RM, Inman DM, et al. Distal axonopathy with structural persistence in glaucomatous neurodegeneration. *Proc Natl Acad Sci U S A*. 2010;107(11):5196-5201.
- Buckingham BP, Inman DM, Lambert W, et al. Progressive ganglion cell degeneration precedes neuronal loss in a mouse model of glaucoma. *J Neurosci*. 2008;28(11):2735-2744.
- Dekeyster E, Aerts J, Valiente-Soriano FJ, et al. Ocular hypertension results in retinotopic alterations in the visual cortex of adult mice. *Curr Eye Res*. 2015;40(12):1269-1283.
- Trivedi V, Bang JW, Parra C, et al. Widespread brain reorganization perturbs visuomotor coordination in early glaucoma. *Sci Rep*. 2019;9(1):14168.
- Lawlor M, Danesh-Meyer H, Levin LA, et al. Glaucoma and the brain: Trans-synaptic degeneration, structural change, and implications for neuroprotection. *Surv Ophthalmol*. 2017.
- Cacabelos R, Caamano J, Gomez MJ, et al. Therapeutic effects of CDP-choline in Alzheimer's disease. Cognition, brain mapping, cerebrovascular hemodynamics, and immune factors. *Ann N Y Acad Sci*. 1996;777:399-403.
- Galletti P, De Rosa M, Cotticelli MG, et al. Biochemical rationale for the use of CDPcholine in traumatic brain injury: pharmacokinetics of the orally administered drug. *J Neurol Sci*. 1991;103 Suppl:S19-S25.
- Skripuletz T, Manzel A, Gropengiesser K, et al. Pivotal role of choline metabolites in remyelination. *Brain*. 2015;138(Pt 2):398-413.
- Alvarez-Sabin J, Santamarina E, Maisterra O, et al. Long-Term Treatment with Citicoline Prevents Cognitive Decline and Predicts a Better Quality of Life after a First Ischemic Stroke. *Int J Mol Sci*. 2016;17(3).
- Schauss AG, Somfai-Relle S, Financsek I, et al. Single- and repeated-dose oral toxicity studies of citicoline free-base (choline cytidine 5'-pyrophosphate) in Sprague-Dawley rats. *Int J Toxicol*. 2009;28(6):479-487.
- Weiss GB. Metabolism and actions of CDP-choline as an endogenous compound and administered exogenously as citicoline. *Life Sci*. 1995;56(9):637-660.
- Secades JJ, Lorenzo JL. Citicoline: pharmacological and clinical review, 2006 update. *Methods Find Exp Clin Pharmacol*. 2006;28 Suppl B:1-56.
- Martinet M, Fonlupt P, Pacheco H et al. Effects of cytidine-5' diphosphocholine on norepinephrine, dopamine and serotonin synthesis in various regions of the rat brain. *Arch Int Pharmacodyn Ther*. 1979;239(1):52-61.
- Gao X, Wang Y, Sun G et al. High dietary choline and betaine intake is associated with low insulin resistance in the Newfoundland population. *Nutrition*. 2017;33:28-34.
- Matteucci A, Varano M, Gaddini L, et al. Neuroprotective effects of citicoline in in vitro models of retinal neurodegeneration. *Int J Mol Sci*. 2014;15(4):6286-6297.
- Chun YH, Han K, Park SH, et al. Insulin resistance is associated with intraocular pressure elevation in a non-obese Korean population. *PLoS One*. 2015;10(1):e112929.
- Fujiwara K, Yasuda M, Ninomiya T, et al. Insulin Resistance Is a Risk Factor for Increased Intraocular Pressure: The Hisayama Study. *Invest Ophthalmol Vis Sci*. 2015;56(13):7983-7987.
- Oh SW, Lee S, Park C, et al. Elevated intraocular pressure is associated with insulin resistance and metabolic syndrome. *Diabetes Metab Res Rev*. 2005;21(5):434-440.
- Faiq MA, Wollstein G, Schuman JS et al. Cholinergic nervous system and glaucoma: From basic science to clinical applications. *Prog Retin Eye Res*. 2019;72:100767.
- Adibhatla RM, Hatcher JF, Dempsey RJ. Citicoline: neuroprotective mechanisms in cerebral ischemia. *J Neurochem*. 2002;80(1):12-23.
- Ottobelli L, Manni GL, Centofanti M, et al. Citicoline oral solution in glaucoma: is there a role in slowing disease progression? *Ophthalmologica*. 2013;229(4):219-226.
- Parisi V. Electrophysiological assessment of glaucomatous visual dysfunction during treatment with cytidine-5'-diphosphocholine (citicoline): a study of 8 years of follow-up. *Doc Ophthalmol*. 2005;110(1):91-102.
- Parisi V, Coppola G, Centofanti M, et al. Evidence of the neuroprotective role of citicoline in glaucoma patients. *Prog Brain Res*. 2008;173:541-554.
- Parisi V, Coppola G, Ziccardi L et al. Cytidine-5'-diphosphocholine (Citicoline): a pilot study in patients with non-arteritic ischaemic optic neuropathy. *Eur J Neurol*. 2008;15(5):465-474.
- Parisi V, Manni G, Colacino G et al. Cytidine-5'-diphosphocholine (citicoline) improves retinal and cortical responses in patients with glaucoma. *Ophthalmology*. 1999;106(6):1126-1134.

34. Pecori Giralaldi J, Virno M, Covelli G et al. Therapeutic value of citicoline in the treatment of glaucoma (computerized and automated perimetric investigation). *Int Ophthalmol*. 1989;13(1-2):109-112.
35. Rejda R, Toczolowski J, Kurkowski J, et al. Oral citicoline treatment improves visual pathway function in glaucoma. *Med Sci Monit*. 2003;9(3):PI24-PI28.
36. Roberti G, Tanga L, Parisi V, et al. A preliminary study of the neuroprotective role of citicoline eye drops in glaucomatous optic neuropathy. *Indian J Ophthalmol*. 2014;62(5):549-553.
37. Virno M, Pecori-Giralaldi J, Liguori A et al. The protective effect of citicoline on the progression of the perimetric defects in glaucomatous patients (perimetric study with a 10-year follow-up). *Acta Ophthalmol Scand Suppl*. 2000(232):56-57.
38. Rossetti L, Jester M, Tranchina L, et al. Can Treatment With Citicoline Eyedrops Reduce Progression in Glaucoma? The Results of a Randomized Placebo-controlled Clinical Trial. *J Glaucoma*. 2020;29(7):513-520.
39. Gandolfi S, Marchini G, Caporossi A, et al. Cytidine 5'-Diphosphocholine (Citicoline): Evidence for a Neuroprotective Role in Glaucoma. *Nutrients*. 2020;12(3).
40. Parisi V, Barbano L, Di Renzo A et al. Neuroenhancement and neuroprotection by oral solution citicoline in non-arteritic ischemic optic neuropathy as a model of neurodegeneration: A randomized pilot study. *PLoS One*. 2019;14(7):e0220435.
41. Oshitari T, Fujimoto N, Adachi-Usami E. Citicoline has a protective effect on damaged retinal ganglion cells in mouse culture retina. *Neuroreport*. 2002;13(16):2109-2111.
42. Schuettauf F, Rejda R, Thaler S, et al. Citicoline and lithium rescue retinal ganglion cells following partial optic nerve crush in the rat. *Exp Eye Res*. 2006;83(5):1128-1134.
43. Galletti P, De Rosa M, Nappi MA, et al. Transport and metabolism of double-labelled CDPcholine in mammalian tissues. *Biochem Pharmacol*. 1985;34(23):4121-4130.
44. Xu J, Sun SW, Naismith RT, et al. Assessing optic nerve pathology with diffusion MRI: from mouse to human. *NMR Biomed*. 2008;21(9):928-940.
45. Henkelman RM, Stanisz GJ, Graham SJ. Magnetization transfer in MRI: a review. *NMR Biomed*. 2001;14(2):57-64.
46. Pawela CP, Biswal BB, Cho YR, et al. Resting-state functional connectivity of the rat brain. *Magn Reson Med*. 2008;59(5):1021-1029.
47. Chan KC, So KF, Wu EX. Proton magnetic resonance spectroscopy revealed choline reduction in the visual cortex in an experimental model of chronic glaucoma. *Exp Eye Res*. 2009;88(1):65-70.
48. Chan KC, Yu Y, Ng SH, et al. Intracameral injection of a chemically cross-linked hydrogel to study chronic neurodegeneration in glaucoma. *Acta Biomater*. 2019;94:219-231.
49. Yu Y, Chau Y. Formulation of in situ chemically cross-linked hydrogel depots for protein release: from the blob model perspective. *Biomacromolecules*. 2015;16(1):56-65.
50. Yu Y, Chau Y. One-step "click" method for generating vinyl sulfone groups on hydroxyl-containing water-soluble polymers. *Biomacromolecules*. 2012;13(3):937-942.
51. Douglas RM, Alam NM, Silver BD, et al. Independent visual threshold measurements in the two eyes of freely moving rats and mice using a virtual-reality optokinetic system. *Vis Neurosci*. 2005;22(5):677-684.
52. Deng W, Faiq MA, Liu C et al. Applications of Manganese-Enhanced Magnetic Resonance Imaging in Ophthalmology and Visual Neuroscience. *Front Neural Circuit*. 2019;13(35).
53. Farber SA, Savci V, Wei A et al. Choline's phosphorylation in rat striatal slices is regulated by the activity of cholinergic neurons. *Brain Res*. 1996;723(1-2):90-99.
54. Mlynarik V, Gambarota G, Frenkel H et al. Localized short-echo-time proton MR spectroscopy with full signal-intensity acquisition. *Magn Reson Med*. 2006;56(5):965-970.
55. Paxinos G, Watson C. *The Rat Brain in Stereotaxic Coordinates: Hard Cover Edition*: Elsevier Science; 2006.
56. Stefan D, Di Cesare F, Andrasescu A, et al. Quantitation of magnetic resonance spectroscopy signals: the jMRUI software package. *Meas Sci Technol*. 2009;20(10).
57. Naressi A, Couturier C, Devos JM, et al. Java-based graphical user interface for the MRUI quantitation package. *Magn Reson Mater Phys*. 2001;12(2-3):141-152.
58. Cudalbu C, Cavassila S, Rabeson H et al. Influence of measured and simulated basis sets on metabolite concentration estimates. *NMR Biomed*. 2008;21(6):627-636.
59. Caprioli J, de Leon JM, Azarod P, et al. Trabeculectomy Can Improve Long-Term Visual Function in Glaucoma. *Ophthalmology*. 2016;123(1):117-128.
60. Aptel F, Bron AM, Lachkar Y et al. Change in Visual Field Progression Following Treatment Escalation in Primary Open-angle Glaucoma. *J Glaucoma*. 2017;26(10):875-880.
61. Aung WY, Mar S, Benzinger TL. Diffusion tensor MRI as a biomarker in axonal and myelin damage. *Imaging Med*. 2013;5(5):427-440.
62. Son JL, Soto I, Oglesby E, et al. Glaucomatous optic nerve injury involves early astrocyte reactivity and late oligodendrocyte loss. *Glia*. 2010;58(7):780-789.
63. You Y, Joseph C, Wang C, et al. Demyelination precedes axonal loss in the transneuronal spread of human neurodegenerative disease. *Brain*. 2019;142(2):426-442.
64. Chan KC, Fu QL, Hui ES et al. Evaluation of the retina and optic nerve in a rat model of chronic glaucoma using in vivo manganese-enhanced magnetic resonance imaging. *Neuroimage*. 2008;40(3):1166-1174.
65. Chan KC, Li J, Kau P, et al. In vivo retinotopic mapping of superior colliculus using manganese-enhanced magnetic resonance imaging. *Neuroimage*. 2011;54(1):389-395.
66. Thuen M, Singstad TE, Pedersen TB, et al. Manganese-enhanced MRI of the optic visual pathway and optic nerve injury in adult rats. *J Magn Reson Imaging*. 2005;22(4):492-500.
67. Ho LC, Wang B, Conner IP, et al. In Vivo Evaluation of White Matter Integrity and Anterograde Transport in Visual System After Excitotoxic Retinal Injury With Multimodal MRI and OCT. *Invest Ophthalmol Vis Sci*. 2015;56(6):3788-800.
68. Fieremans E, Jensen JH, Helpert JA. White matter characterization with diffusional kurtosis imaging. *Neuroimage*. 2011;58(1):177-188.
69. Wang X, Cusick MF, Wang Y, et al. Diffusion basis spectrum imaging detects and distinguishes coexisting subclinical inflammation, demyelination and axonal injury in experimental autoimmune encephalomyelitis mice. *NMR in Biomedicine*. 2014;27(7):843-852.
70. Bukhari SM, Kiu KY, Thambiraja R, et al. Microvascular endothelial function and severity of primary open angle glaucoma. *Eye (Lond)*. 2016;30(12):1579-1587.
71. Kaiser HJ, Flammer J, Wenk M et al. Endothelin-1 plasma levels in normal-tension glaucoma: abnormal response to postural changes. *Graefes Arch Clin Exp Ophthalmol*. 1995;233(8):484-488.
72. Kornzweig AL, Eliasoph I, Feldstein M. Selective atrophy of the radial peripapillary capillaries in chronic glaucoma. *Arch Ophthalmol*. 1968;80(6):696-702.
73. Almasieh M, MacIntyre JN, Pouliot M, et al. Acetylcholinesterase inhibition promotes retinal vasoprotection and increases ocular blood flow in experimental glaucoma. *Invest Ophthalmol Vis Sci*. 2013;54(5):3171-3183.

74. Hetu S, Pouliot M, Cordahi G, et al. Assessment of retinal and choroidal blood flow changes using laser Doppler flowmetry in rats. *Curr Eye Res.* 2013;38(1):158-167.
75. Grunwald JE, Riva CE, Stone RA, et al. Retinal autoregulation in open-angle glaucoma. *Ophthalmology.* 1984;91(12):1690-1694.
76. Schmidl D, Garhofer G, Schmetterer L. The complex interaction between ocular perfusion pressure and ocular blood flow - relevance for glaucoma. *Exp Eye Res.* 2011;93(2):141-155.
77. Cherecheanu AP, Garhofer G, Schmidl D, et al. Ocular perfusion pressure and ocular blood flow in glaucoma. *Curr Opin Pharmacol.* 2013;13(1):36-42.
78. Grunwald JE, Piltz J, Hariprasad SM, et al. Optic nerve and choroidal circulation in glaucoma. *Invest Ophthalmol Vis Sci.* 1998;39(12):2329-2336.
79. Michelson G, Langhans MJ, Groh MJ. Perfusion of the juxtapapillary retina and the neuroretinal rim area in primary open angle glaucoma. *J Glaucoma.* 1996;5(2):91-98.
80. Amerasinghe N, Aung T, Cheung N, et al. Evidence of retinal vascular narrowing in glaucomatous eyes in an Asian population. *Invest Ophthalmol Vis Sci.* 2008;49(12):5397-5402.
81. Tezel G, Kass MA, Kolker AE, et al. Plasma and aqueous humor endothelin levels in primary open-angle glaucoma. *J Glaucoma.* 1997;6(2):83-89.
82. Meerson A, Cacheaux L, Goosens KA, et al. Changes in brain MicroRNAs contribute to cholinergic stress reactions. *J Mol Neurosci.* 2010;40(1-2):47-55.
83. Walker SW, Strachan MW, Lightly ER, et al. Acetylcholine stimulates cortisol secretion through the M3 muscarinic receptor linked to a polyphosphoinositide-specific phospholipase C in bovine adrenal fasciculata/reticularis cells. *Mol Cell Endocrinol.* 1990;72(3):227-238.
84. Buckley C, Hadoke PW, Henry E, et al. Systemic vascular endothelial cell dysfunction in normal pressure glaucoma. *Br J Ophthalmol.* 2002;86(2):227-232.
85. Flammer J, Konieczka K. The discovery of the Flammer syndrome: a historical and personal perspective. *EPMA J.* 2017;8(2):75-97.
86. Dada T, Mittal D, Mohanty K, et al. Mindfulness Meditation Reduces Intraocular Pressure, Lowers Stress Biomarkers and Modulates Gene Expression in Glaucoma: A Randomized Controlled Trial. *J Glaucoma.* 2018;27(12):1061-1067.
87. Sabel BA, Flammer J, Merabet LB. Residual vision activation and the brain-eye-vascular triad: Dysregulation, plasticity and restoration in low vision and blindness - a review. *Restor Neurol Neurosci.* 2018;36(6):767-791.
88. Hombrebueno JR, Luo C, Guo L, et al. Intravitreal Injection of Normal Saline Induces Retinal Degeneration in the C57BL/6J Mouse. *Transl Vis Sci Technol.* 2014;3(2):3.
89. Frezzotti P, Giorgio A, Motolese I, et al. Structural and functional brain changes beyond visual system in patients with advanced glaucoma. *PLoS One.* 2014;9(8):e105931.
90. Klaassens BL, Rombouts SA, Winkler AM, et al. Time related effects on functional brain connectivity after serotonergic and cholinergic neuromodulation. *Hum Brain Mapp.* 2016.
91. Chamoun M, Groleau M, Bhat M, et al. Dose-dependent effect of donepezil administration on long-term enhancement of visually evoked potentials and cholinergic receptor overexpression in rat visual cortex. *J Physiol Paris.* 2016;110(1-2):65-74.
92. Chamoun M, Sergeeva EG, Henrich-Noack P, et al. Cholinergic Potentiation of Restoration of Visual Function after Optic Nerve Damage in Rats. *Neural Plast.* 2017;2017:6928489.
93. Ulus IH, Watkins CJ, Cansev M, et al. Cytidine and uridine increase striatal CDP-choline levels without decreasing acetylcholine synthesis or release. *Cell Mol Neurobiol.* 2006;26(4-6):563-577.
94. Iulia C, Ruxandra T, Costin LB, et al. Citicoline - a neuroprotector with proven effects on glaucomatous disease. *Rom J Ophthalmol.* 2017;61(3):152-158.
95. Blusztajn JK, Holbrook PG, Lakher M, et al. "Autocannibalism" of membrane choline-phospholipids: physiology and pathology. *Psychopharmacol Bull.* 1986;22(3):781-786.
96. Dewundara SS, Wiggs JL, Sullivan DA, et al. Is Estrogen a Therapeutic Target for Glaucoma? *Semin Ophthalmol.* 2016;31(1-2):140-146.
97. Qureshi IA. Intraocular pressure: association with menstrual cycle, pregnancy and menopause in apparently healthy women. *Chin J Physiol.* 1995;38(4):229-234.
98. Harada C, Kimura A, Guo X, et al. Recent advances in genetically modified animal models of glaucoma and their roles in drug repositioning. *Br J Ophthalmol.* 2019;103(2):161-166.

Publisher's Note Springer Nature remains neutral with regard to jurisdictional claims in published maps and institutional affiliations.